THEORY, DESIGN, AND PERFORMANCE OF A COAXIAL, EXPLODING-WIRE SYSTEM

By

JERRY ALLEN YODER II

Bachelor of Arts

Oklahoma City University

Oklahoma City, Oklahoma

1964

Submitted to the Faculty of the Graduate College
of the Oklahoma State University
in partial fulfillment of the requirements
for the Degree of
MASTER OF SCIENCE
May, 1970

THEORY, DESIGN, AND PERFORMANCE OF A

COAXIAL, EXPLODING-WIRE SYSTEM

Thesis Approved:

Francis C. Todd
Thesis Adviser

D. Durham
Dean of the Graduate College

PREFACE

This work was undertaken at the suggestion of Dr. F. C. Todd who acted as the author's project adviser. The purpose of this research was to design and construct an "exploding wire" system to be used in the study of dense, high energy density aluminum plasmas.

The author wishes to thank Dr. Todd for his guidance and counsel which contributed to the completion of this work, and to H. G. Gurney and J. J. Dunn for their assistance in the design and construction of various machined parts. The author also wishes to express gratitude to H. J. Jackson and R. D. Payne who made the initial literature search and began the design of the "exploding wire" system.

A special note of thanks goes to the United States Navy, Bureau of Ships, for supplying diagrams of coaxial connectors which are no longer mass produced.

Part of this work was carried out under NASA Contract NASr-7 and was finished under NASA Contract NAS8-21391. These contracts were administered through the Research Foundation, Oklahoma State University. The author is also indebted to NASA for a fellowship in the form of a NASA Traineeship from September 1964 to September 1967.

TABLE OF CONTENTS

LIST OF TABLES

LIST OF FIGURES

CHAPTER I

INTRODUCTION

In 1966, Bruce presented the evolution in time for the expansion into a vacuum of a small sphere of aluminum plasma. Sufficient initial, uniform energy density was assumed to be added to the aluminum sphere to produce a high density plasma. The results depended upon an analytical equation of state which was developed for the problem. Two results stand out significantly in Bruce's work:

1. The formation of a "cold shell" at the outer edge of the expanding material,
2. The creation of a high temperature, low density core.

Subsequently, Brown (1968) measured the light output as a function of time from a vacuum spark between aluminum electrodes, using a pulsed photomultiplier. The results, which Brown obtained, indicate the formation of a "cold shell" in the expanding aluminum plasma which conducted the current of the spark discharge.

Another way to produce a high energy density, aluminum plasma is the "exploding wire" phenomena. In the published literature, some evidence is presented for the formation of a "cold shell" (Bennett, 1962) and the creation of a "hot core" (Bennett, 1965) in the "exploding wire" phenomena. It thus becomes very desirable to use the "exploding wire" phenomena as a means of checking the theoretical approach of Bruce, using in part, the experimental techniques of Brown. Other tests could

be performed with a far ultraviolet vacuum spectrograph built by Payne (1966) and with a recently constructed quadrupole mass filter (Willis, 1969), for determination of ionization in the aluminum plasma. To properly correlate experiments to the theoretical approach, it is necessary to know accurately the energy content and volume of the wire prior to its expansion.

Kvartskhava et al. (1957) and Thomas and Hearst (1967) have proposed and used methods for measuring the energy content of an "exploding wire" in capacitive discharge systems. These methods can become rather complicated due to the non-linear circuit equations; a simple, yet reliable method of measuring the energy content would be of great worth.

Another problem associated with "exploding wires" is the need to establish a volume for the wire at a time which can be considered as the beginning of the explosion. Before the initial energy density can be determined, this volume must be established. Reithel and Blackburn (1962) have discussed a concept that is known as the "resistance anomaly" in "exploding wire" phenomena. This anomaly expresses the fact that the resistance of a wire of a specific, initial size is not a unique function of the energy content, but depends upon the rate of energy input to the wire. For a higher rate of energy input, the resistance increases at a lower rate. This anomaly was discussed on the basis of a hydrodynamic model and was attributed to inertial confinement in the expansion process. Tucker and Neilson (1959) previously provided a very useful measure of inertial confinement. The noted that for a given material, the integral of the square of the current density with respect to time while the resistance increases to its first peak is a constant. In view of these remarks, it seems highly desirable to insert the energy

into the wire in as short a time as possible. This employs the inertial confinement in order to establish an initial volume at which the explosion begins.

Another problem is to remove the electromagnetic fields after the plasma is formed. In the conventional manner of exploding a wire by discharging a capacitor bank through the wire, electromagnetic fields exist in and around the wire during the expansion of the plasma. This effect does not correspond to the theoretical problem and must be eliminated in order to compare the analytical solution with the experiment.

One might ask the question, is the energy input uniform throughout the "exploding wire" when it is heated by the conducting current. This question is answered in Chapter II. It is shown for a small wire of constant volume that the current first travels on the outer edge of the wire. Within a very few nanoseconds, the current density becomes practically uniform throughout the wire. For times much larger than a nanosecond, the energy is inserted uniformly in the wire provided that no expansion occurs.

The main purpose of this thesis is to discuss the theory and construction of an "exploding wire" system which overcomes, to some extent, the preceeding difficulties. The basic circuitry which appears capable of satisfying the present goals, was found in the published literature (Tucker, 1960). In the system which has been constructed, a square voltage pulse of known amplitude and duration is launched down a coaxial cable which is terminated in the wire to be exploded. The wire is mounted in a vacuum. This pulse is obtained by switching a coaxial cable, pulse generator by means of a pressurized spark gap. A second spark gap is placed just ahead of the wire at the end of the cable in

order to sharpen the leading edge of the voltage pulse. Of course, the wire will not absorb all of the incident energy; part of the energy will be reflected. This reflected energy could enter the wire by multiple reflections at the ends of the coaxial cable, if the energy were not removed from the cable and dissipated. Since it is desirable for the wire to expand in a region free of electromagnetic fields, a timed and triggered spark gap is employed to discharge the excess energy into a coaxially mounted resistor. This system is equivalent, in its basic operation, to that of Tucker, but has the additional features of having the wire mounted in a vacuum and of eliminating the reflected energy. The basic electrical features of the system are presented in Figure 1.

The coaxialized "exploding wire" system which has been constructed has several advantages over the capacitive discharge system:

1. The circuit equations are algebraic rather than non-linear differential equations.
2. A voltage measurement across the wire alone serves to determine the energy content of the wire.
3. By making the system completely coaxialized, good shielding and frequency response is obtained.
4. The wire is mounted as part of the center conductor of a coaxial cable delay line; the resulting cylindrical symmetry serves to stabilize the wire.
5. A coaxialized pulse generator delivers current to the wire for a predetermined period of time, after which the wire is allowed to expand.

Since it is desirable to insert a large amount of energy into a wire in a very short period of time, it is important to use a very small

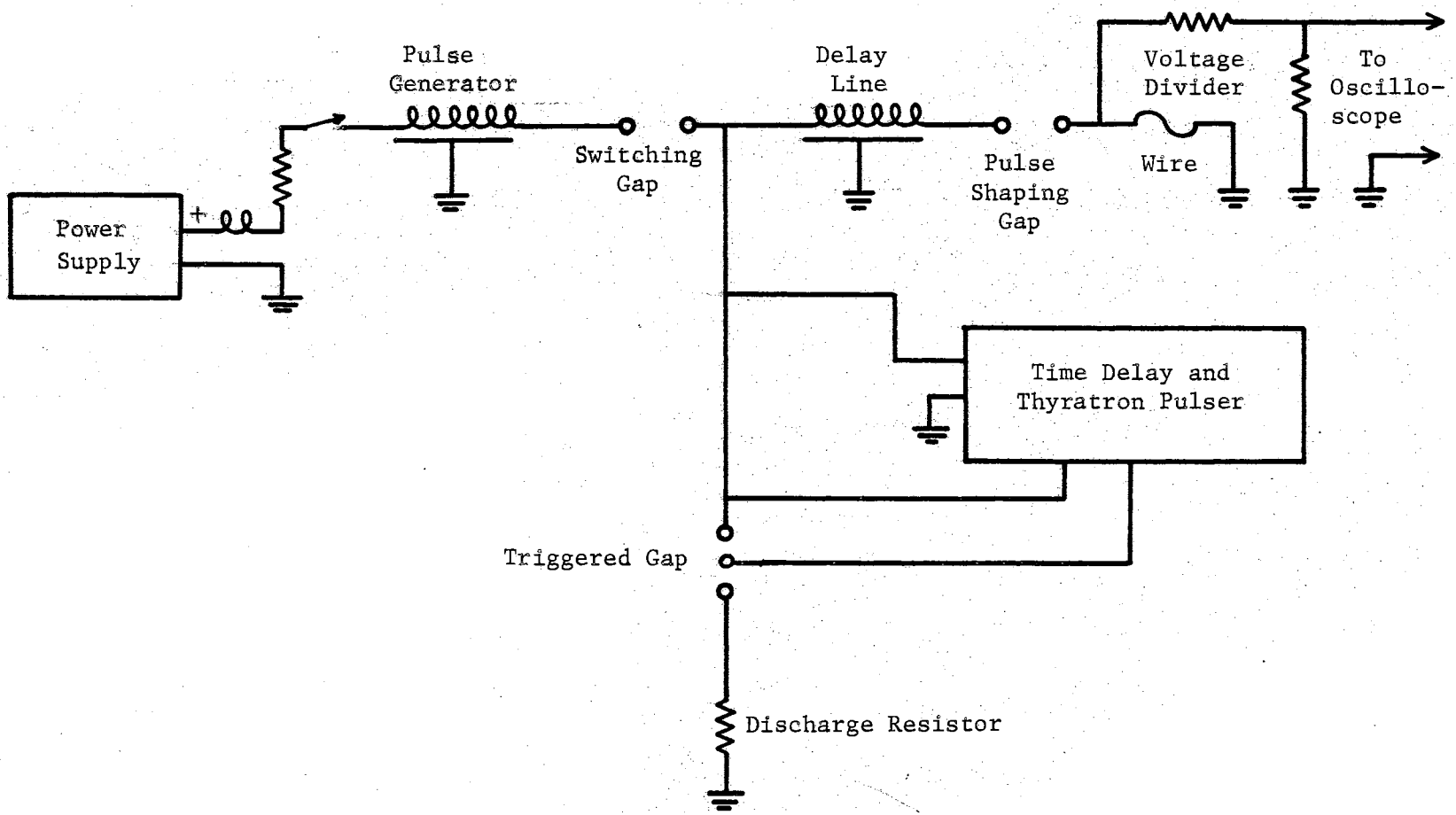

Figure 1. Electrical "Exploding Wire" Circuit

diameter wire. For a given current in the wire, a smaller diameter wire has a greater resistance, and accepts more energy per unit time than a larger diameter wire. The smaller diameter wire also has a greater "pinch" pressure (see Chapter II) which tends to prevent expansion of the wire. The hydrodynamic, "pinch" pressure is proportional to the square of the current density in the wire. Several aspects need to be considered when selecting a size of wire for a current pulse of known amplitude and duration.

A. Wire Length

1. Long enough to minimize end effects.
2. Short enough to appear as a sphere at a few centimeters from the wire.

B. Wire Diameter

1. Small enough compared to the length to minimize end effects.
2. Small enough to be heated to the desired temperature by the available current.
3. Large enough to be handled easily.

The duration of the current pulse to the wire is restricted in several ways:

1. Short enough so the wire remains at essentially constant volume during the energy input.
2. Short enough to prevent arcs from shorting the wire, or conducting vapors.

The remainder of this thesis is devoted to a theoretical discussion of the "pinch effect", to the construction and operation of the completely coaxialized "exploding wire" system, and finally, to some preliminary results that demonstrate the operation of the system.

CHAPTER II

"PINCH EFFECT" IN A SMALL ALUMINUM WIRE

When an electric current flows through a cylindrical wire, the self-produced fields exert forces on the moving charges which are directed toward the center of the wire. These forces result in a radial pressure distribution throughout the cross section of the wire. This pressure distribution tends to squeeze or "pinch" the wire.

The purpose of this chapter is to determine the current density distribution in a small diameter aluminum wire as a function of time. From this distribution, the resulting magnetic induction and pressure distribution will be determined.

The Diffusion Equation

To derive the diffusion equation (Gartenhaus, 1964), first consider Maxwell's electromagnetic equations for a conductor in rationalized MKS units.

$$\nabla \cdot \bar{B} = 0$$

$$\nabla \cdot \bar{E} = 0$$

$$\nabla \times \bar{E} = -\dot{\bar{B}}$$

$$\nabla \times \bar{B} = \mu_o \bar{J},$$

where

$\bar{B}$ = magnetic induction vector

$\bar{E}$ = electric field vector

$\bar{J}$ = electric current density.

It is assumed that no charge density exists within the conductor, and that the displacement current vanishes. The permeability is assumed to have the free space value, μ_o.

In addition to Maxwell's equations, the conductor is assumed to obey Ohm's law in the form,

$$\bar{J} = \sigma\bar{E},$$

where

σ = electrical conductivity.

Taking the curl of the last of Maxwell's equations and using the vector identity,

$$\nabla \times \nabla \times \bar{A} = \nabla(\nabla \cdot \bar{A}) - \nabla^2 \bar{A},$$

appropriate substitutions give the diffusion equation,

$$\dot{\bar{B}} = \nabla^2 \bar{B}/\mu_o\sigma.$$

This equation is solved for $\bar{B}$, and then $\bar{J}$ is determined by the last of Maxwell's equations.

Geometry and Boundary Conditions

Consider a cylindrical conductor of radius r_o, of infinite length, and oriented along the z axis of a cylindrical coordinate system. A current, i, flows along the cylinder. The resulting current density has only a component in the z direction which is a function of the radial distance, r, only. The magnetic induction has only a component in

the $r\,d\theta$ direction which is a function of r only. The following solution for $\bar{B}$ and $\bar{J}$ is given by Anderson et al. (1958).

The diffusion equation, after convertion to cylindrical coordinates, and with the above conditions is written,

$$B'' + B'/r - B/r^2 = \mu_o \sigma B,$$

where

$$B = \text{tangential component of } \bar{B}$$

According to the "skin effect" (Francis, 1960), the current first travels on the outer surface of the conductor and then diffuses toward the center. The boundary conditions for B, corresponding to this situation, are

$$B(r,o) = 0 \; ; \; r < r_o$$

$$B(r_o,t) = B_o \; ; \; t > 0,$$

where B_o is the constant value of B at the surface of the conductor.

Solution of the Diffusion Equation

Employing the substitution

$$B(r,t) = U(r,t) + V(r).$$

the following is obtained,

$$U'' + U'/r - U/r^2 = \mu_o \sigma U$$

$$V'' + V'/r - V/r^2 = 0,$$

with boundary conditions

$$U(r,0) = - V(r)$$

$$U(r_o,t) = 0 \; ; \; t > 0$$

$$V(r_o) = B_o \; .$$

The equation for V is an Euler's equation (Kells, 1960). The solution, after applying the boundary condition and imposing the restriction that V be finite at r = 0, is

$$V = B_o \, x$$

$$x = r/r_o \; .$$

Separating the radial and time dependence by the substitution,

$$U(r,t) = S(r) \, T(t),$$

results in the following:

$$T' + \mu_o \sigma \, T/\lambda^2 = 0$$

$$r^2 \, S'' + rS' + (\lambda^2 \, r^2 - 1) \, S = 0$$

$$\lambda^2 = \text{undetermined constant} \; .$$

The equation for T is readily solved.

$$T = \exp(-\lambda^2 \, t/\mu_o \sigma) \; .$$

The equation for S may be solved by making the substitution,

$$W = \lambda r,$$

to obtain

$$W^2 \, S'' + W \, S' + (W^2 - 1) \, S = 0.$$

This is a Bessel's function of order one (Kells, 1960). Its solution is

$$S = \sum_{n=1}^{\infty} A_n \, J_1 \, (W_n)$$

$$W_n = \lambda_n r$$

$J_1(W_n)$ = Bessel function of order one

By collecting terms, the solution for U(r,t) is

$$U(r,t) = \sum_{n=1}^{\infty} A_n J_1(W_n) \exp(-\lambda^2 t/\mu_o\sigma).$$

From the boundary condition at $r = r_o$ for $t < 0$,

$$J_1(a_n) = 0$$

where,

$$a_n = \lambda_n r_o .$$

We can now write U as a function of the relative coordinate x.

$$U(x,t) = \sum_{n=1}^{\infty} A_n J_1(a_n x) \exp(-a_n^2 t/r_o^2 \mu_o\sigma).$$

To evaluate the A_n, the boundary condition at $t = 0$ is applied to obtain

$$U(r,0) = \sum_{n=1}^{\infty} A_n J_1(a_n x) = -B_o x$$

Multiplying this last expression by $x J_1(a_m x)$ and integrating with respect to x between 0 and 1, using the orthogonality conditions for Bessel functions (see Appendix A),

$$A_n = 2 B_o/a_n J_o(a_n)$$

$J_o(a_n)$ = Bessel function of order zero.

The solution for the magnetic induction thus becomes

$$B(x,t) = B_o [x + 2 \sum_{n=1}^{\infty} J_1(a_n x) \exp(- a_n^2 t/r_o^2 \mu_o \sigma)/a_n J_o(a_n)].$$

In the actual calculation for the magnetic induction, this last expression will not be used. Rather, B is calculated from J by an appropriate integration. In this way the use of Bessel functions of two different orders will be avoided, which saves considerable computer time. Upon integrating the last of Maxwell's equations using Stokes' theorm, one obtains for the present situation

$$B(r) = \mu_o/r \int_0^r J\, r\, dr \; ; \; r \neq 0$$

$$B(0) = 0$$

The solution for the current density is obtained by using the equations

$$\bar{J} = [\nabla \times \bar{B}]/\mu_o$$

$$J(r) = [B/r + B']/\mu_o$$

$$J = z \text{ component of } \bar{J},$$

or, in terms of x,

$$J(x) = [B/x + B']/r_o \mu_o .$$

The equation for the current density is

$$J(x,t) = \gamma[1 + \sum_{n=1}^{\infty} J_o(a_n x) \exp(- a_n^2 t/r_o^2 \mu_o \sigma)/J_o(a_n)]$$

$$\gamma = 2 B_o/r_o \mu_o .$$

The "Pinch" Pressure

For an infinitely long, uniform cylindrical conductor which has a uniform current density distribution, Hague (1962) presented arguments establishing the "pinch" pressure as a function of the radial distance. Similar arguments allow for an arbitrary current density distribution in the conductor.

Consider a volume element, $\delta\Omega$, which is at a distance, r, from the center of the conductor

$$\delta\Omega = r\,\delta r\,\delta\theta\,\delta 1$$

$$1 = \text{conductor length.}$$

The force F_c on a single charged particle in $\delta\Omega$ is

$$\bar{F}_c = q[\bar{v} \times \bar{B}],$$

where

$$q = \text{charge of the current carrier}$$

$$\bar{v} = \text{velocity of the current carrier}$$

This last equation is indicative of the fact that the force on a charged particle is directed radially inward. For the present situation this equation reduces to

$$|\bar{F}_c| = q\,v\,B$$

$$v = z \text{ component of } \bar{v}\ .$$

The force δF per unit volume $\delta\Omega$ is

$$\delta F/r\,\delta r\,\delta\theta\,\delta 1 = |\bar{F}_c|\,n\ ,$$

where

$$n = \text{number density of current carriers .}$$

Thus,

$$\delta F = n\, q\, v\, B\, r\, \delta r\, \delta\theta\, \delta l,$$

where v is now an average velocity for the current carriers. But the current density is given by

$$J = n\, q\, v,$$

so that,

$$\delta F = J\, B\, r\, \delta r\, \delta\theta\, \delta l.$$

The force δF is exerted on the area $r\, \delta\theta\, \delta l$; hence, the ring of radius r and thickness δr experiences a pressure differential δP given by

$$\delta P = \delta F / r\, \delta\theta\, \delta r = J\, B\, \delta r$$

The total pressure at a distance, r, from the center of the conductor is obtained by integrating P from r to the surface of the conductor.

$$P(r) = \int_{r}^{r_o} J\, B\, dr$$

It should be realized that this result implies that pressure effects are instantaneous. In actuality, pressure effects are expected to propagate at the velocity of sound in the conductor. This requires a more complicated set of equations than those for the present problem.

The Computer Solution

In order to prepare the equations for J, B, and P to be solved on

a computer, it was decided to avoid absolute values by defining relative values for all of the variables. In addition to the relative coordinate, x, which has already been defined, the following are also defined:

$$I = J/I_o$$

$$I_o = i/\pi r_o^2 = \text{current density when it is uniform}$$

$$M = B/B(r_o)$$

$$B(r_o) = \mu_o\, i/2\,\pi\, r_o$$

$$= \text{constant magnetic induction at surface of conductor}$$

$$Q = P/P_o$$

$$P_o = \mu_o\, i^2/4\pi^2\, r_o^2$$

$$= \text{pressure at } r = 0 \text{ for uniform current density.}$$

Using these definitions, the equation to be solved become

$$I(x,t) = 1 + \sum_{n=1}^{\infty} J_o(a_n\, x)\, \exp(-\, a_n^2\, t/r_o^2\, \mu_o \sigma)/J_o(a_n)$$

$$M(x,t) \quad 2/x \int_0^x I\, x\, dx \; ; \; x < 0$$

$$M(0,t) = 0$$

$$Q(x,t) = 2 \int_x^1 I\, M\, dx$$

These equation were solved on an IBM 360/50 computer which is available at Oklahoma State University. The following parameters are used for an aluminum conductor.

$$r_o = 1.27 \times 10^{-5} \text{ m}$$

$$\sigma = 3.57 \times 10^{7} \text{ mho/m} \quad @ \ 20^{\circ}\text{C}$$

$$\mu_o = 4\pi \times 10^{-7} \text{ hy/m} .$$

The results of the computer calculations appear in Figures 2, 3, and 4. A polynomial approximation is used for the Bessel functions of order zero. This approximation is given in Appendix B. The zeros of the Bessel functions of order one were obtained from the tables of Jahnke and Emde (1943). The series expansion for I converged very rapidly. As a result it was found necessary to use only ten terms of the expansion.

The values of I, M, and Q at $t = 0$ and at $t = \infty$ are of particular interest in checking the computer solution. At $t = 0$, the current flows entirely on the surface of the conductor and may be represented by

$$I)x,0) = \tfrac{1}{2}\,\delta(x - 1) .$$

Consequently,

$$M(x,0) = 0 \ ; \ x < 1$$

$$M(1,0) = 1 .$$

In order to obtain Q at $t = 0$, a delta function, multiplied by M, is integrated. This integral has a discontinuity of magnitude 1 at $x = 1$. If M were written in a Fourier series it would converge to $\frac{1}{2}$ at $x = 1$. This value is the one assumed to be valid for use with the delta function when integrating at $x = 1$. As a result, the following value is obtained:

$$Q(x,0) = \tfrac{1}{2}$$

This value for Q is in agreement with the calculations of Van Kampen and Felderhof (1967) who use a slightly different approach to the problem. It is further substantiated by the computer solution for times near $t = 0$. At $t = \infty$, the following is obtained:

$$I(x,\infty) = 1$$

$$M(x,\infty) = x$$

$$Q(x,\infty) = 1 - x^2$$

The quantity $r_o^2 \mu_o \sigma$ should give some indication of the time need for the current density to become uniform throughout the conductor. In the case of a 0.001 inches diameter wire, a calculation shows

$$r_o^2 \mu_o \sigma = 7.24 \text{ nanosec.}$$

The computer solution shows that the current density becomes essentially uniform after about 2.5 nanoseconds. An expression may be written that is valid for any cylindrical conductor. The approximate time, t_o, is required to obtain a uniform current density distribution.

$$t_o = r_o^2 \mu_o \sigma / 3$$

As stated earlier, the pressure effects in the conductor were assumed to be instantaneous. This assumption is now investigated further. The velocity of propagation, v_L, of a plane longitudinal wave in bulk aluminum is

$$v_L = 6.42 \times 10^3 \text{ m/sec}$$

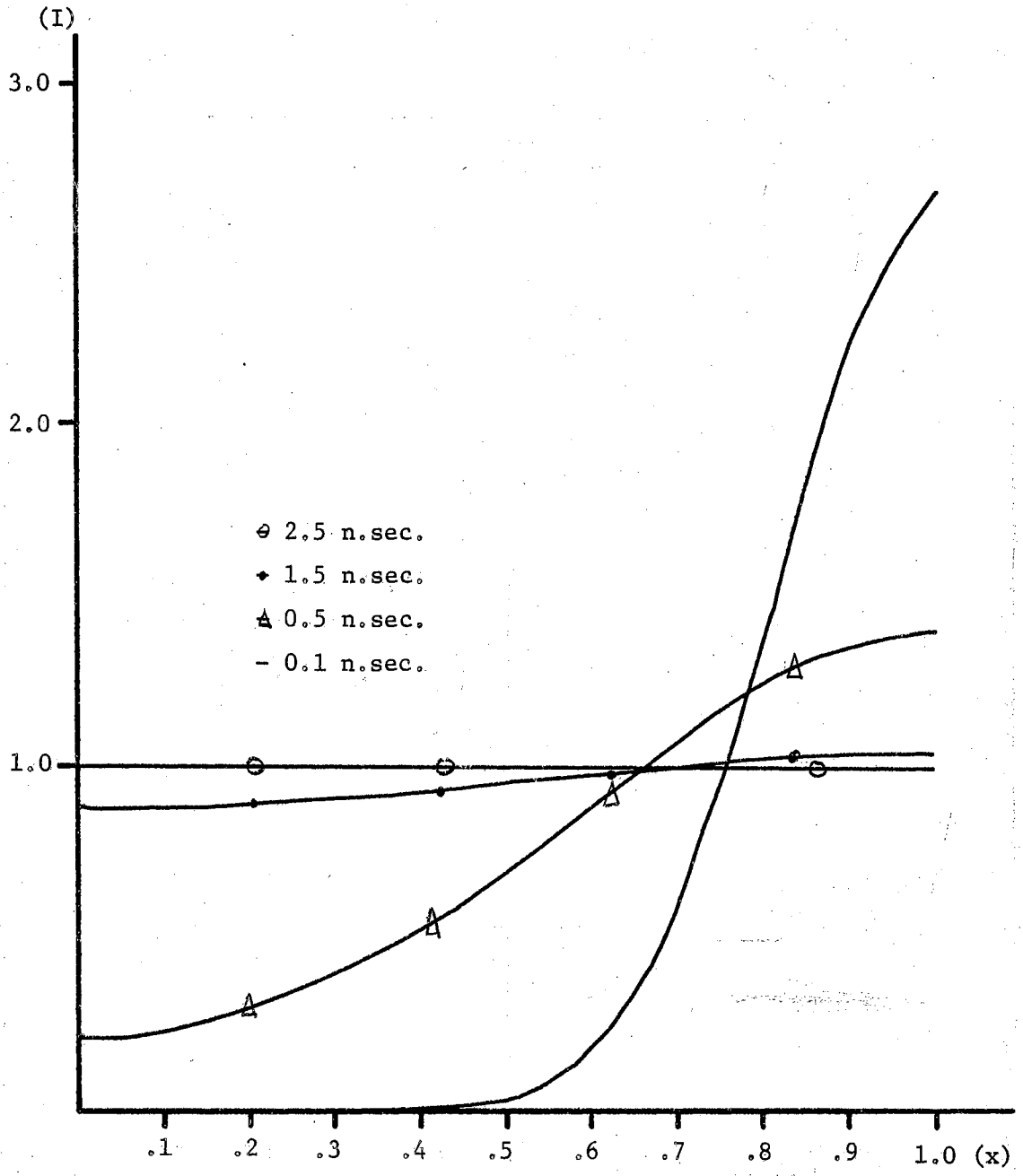

Figure 2. Computer Solution for the Current Density

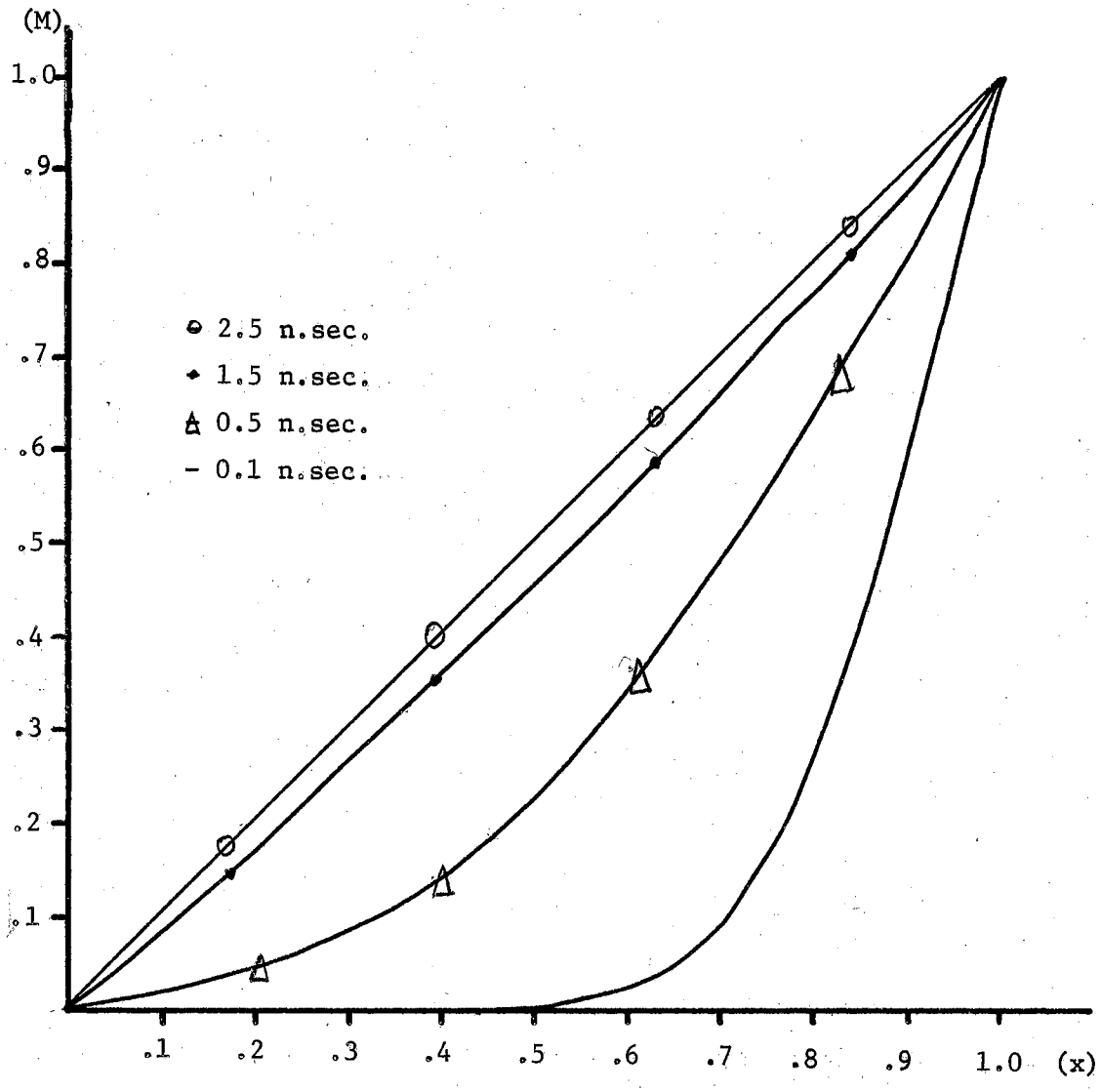

Figure 3. Computer Solution for the Magnetic Induction

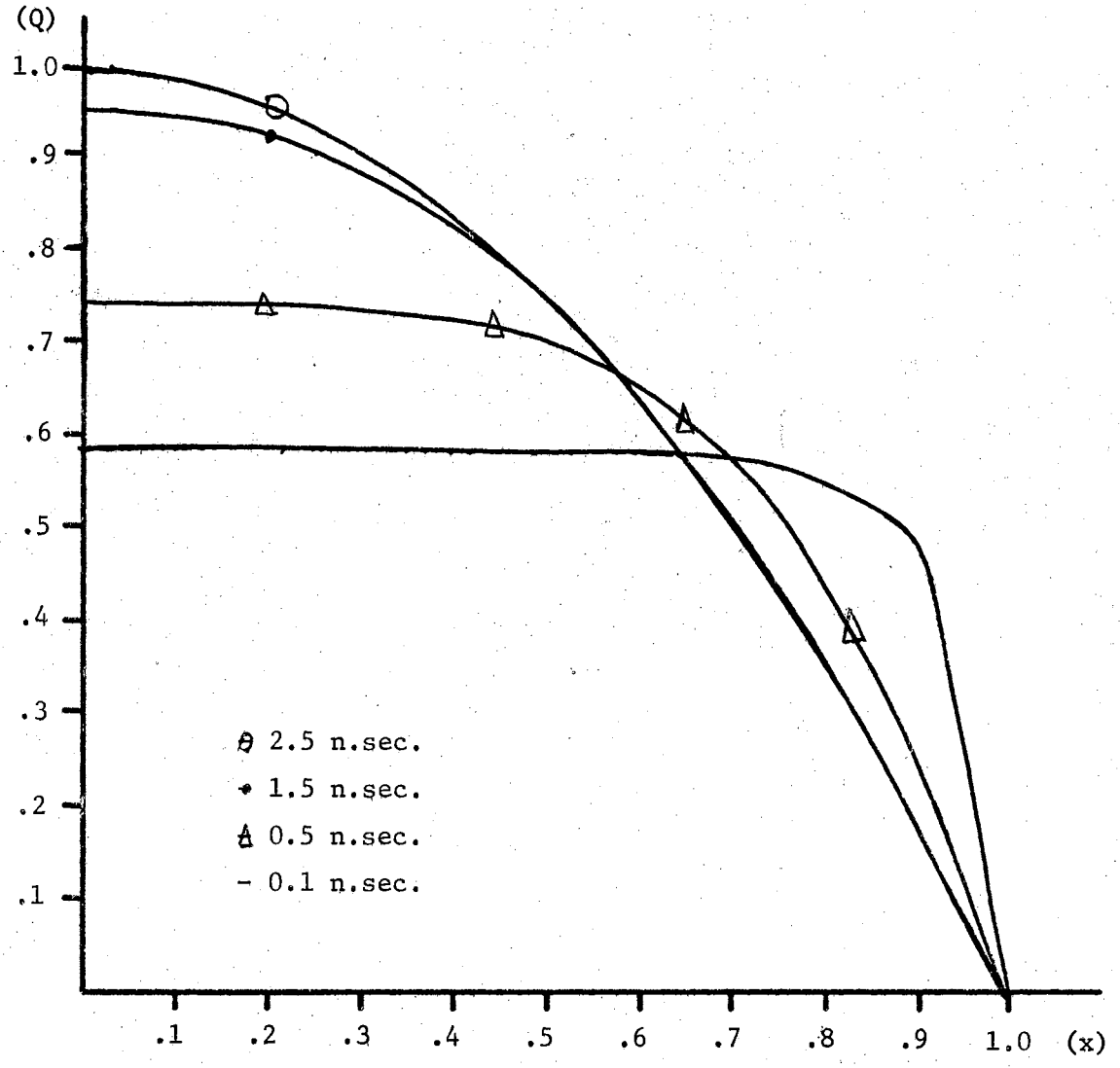

Figure 4. Computer Solution for the "Pinch" Pressure

A pressure wave which travels from the outer edge of the conductor to the center requires a time t_L, where

$$t_L = r_o/v_L .$$

By equating t_o and t_L, we can find a conductor radius R for which the electromagnetic and pressure effects, in some sense, propagate with the same velocity.

$$R = 3/\mu_o \sigma v_L$$

For aluminum we have

$$R = 1.07 \times 10^{-5} \text{ m}$$

The above discussion indicates the formation and propagation of a shock wave in the wire. It should be realized, that in an actual situation, the current cannot rise instantaneously on the surface of the wire. This "shock effect" is, therefore, less than what it might appear. It is desirable to indicate the magnitude of the "pinch" pressures which may be encountered for a 0.001 inches aluminum wire. For this purpose, Table I presents values of P_o for various currents.

As a conclusion to this chapter, a simple calculation indicates the order of magnitude of the compression for a wire, which is expected from the "pinch effect". The isothermal compressibility, k, (King, 1962), is defined by the following equation:

$$k = - (1/V) (\partial V/\partial P),$$

where

V = volume

P = pressure .

Thermal effects are not considered since they would tend to expand the wire rather than compress it. Compressional effects are calculated for the initial instant before the temperature starts to rise. The equation for the compressibility is rewritten in terms of the mass density ρ.

$$k = (1/\rho)(\partial\rho/\partial P)$$

Assuming k to be constant, this equation may be integrated in the following manner:

$$k \int_{P}^{P+\Delta P} dP = \int_{\rho_o}^{\rho} d\rho/\rho$$

$$k\,\Delta P = \mathrm{Ln}(\rho/\rho_o)$$

By letting

$$\Delta P = P_o/2 ,$$

the following equation is obtained:

$$\rho/\rho_o = \exp(k\,P_o/2)$$

Since the compressibilities for solid conductors are so small, the following approximation is made:

$$\rho/\rho_o = 1 + k\,P_o/2 .$$

The isothermal compressibility for aluminum is

$$(k)_{Al} = 1.37 \times 10^{-14} \ m^2/nt \qquad @ \ 20^{\circ}C$$

Values for the compression ratio ρ/ρ_o are presented in Table I. It is obvious that the effect is very small.

TABLE I

PRESSURE EFFECTS IN A 0.001 INCHES DIAMETER ALUMINUM WIRE

i (amperes)	P_o (nt/m^2)	ρ/ρ_o
10.	1.97×10^4	1.000000000135
100.	1.97×10^6	1.0000000135
1000.	1.97×10^8	1.00000135
2000.	3.94×10^8	1.00000270

CHAPTER III

COAXIAL CABLE THEORY

In this chapter, the characteristics of coaxial cables are reviewed and their application to obtain a pulse generator is presented. This summary emphasizes the importance of the coaxial cable in the assembly of the "exploding wire" facility. The presented equations are taken from the development of the subject by Millman and Taub (1956), Whitmer (1962), and Frungel (1965). This chapter includes the development of the equations which relate the voltage across the wire to its resistance and to the energy input to the wire and the resulting plasma. In conclusion, a short description is presented of circuits of cables that may be employed to increase the input of energy to the "exploding wire".

The Coaxial Cable as a Delay Line

Delay lines are passive, four-terminal networks which have the property that a signal applied to the input terminals appears at the output terminals after a time interval, T, which is called the delay time. If a signal is applied to a practical delay line, the signal will suffer distortion and attenuation. In this case, the delay time is defined as the time interval between the 50 per cent amplitude points of the rising edge of the incident and of the delayed signals.

The coaxial cable delay line is of particular interest for the problem that is considered in this thesis. It is practical to use a

coaxial cable as a delay line since its electrical parameters are distributed; that is, the coaxial cable has a capacitance, C_L, and an inductance, H_L, per unit length. Physically, the coaxial cable consists of two concentric, cylindrical conductors with diameters A and B, which are insulated by a dielectric of high electrical resistance. The geometry of a section of coaxial cable and its equivalent, electrical circuit are sketched in Figure 5. Between the two conductors, the insulating material has a dielectric constant, k.

An important parameter of the coaxial cable is its characteristic impedance, which is defined by the relation,

$$R_o = \sqrt{H_L/C_L},$$

where R_o has the units of electrical resistance. If an ideal cable is terminated by a non-inductive resistance which has the same value as its characteristic impedance, the output signal will show no distortion of input signal at the output terminals. In particular, there is not distortion of a complex wave. According to electromagnetic theory, a siunsoidal voltage that is applied to the input terminals of a cable will travel toward the output terminals with a constant velocity of propagation, v, which is independent of frequency. Since any wave form can be resolved into its Fourier spectrum, an ideal coaxial cable that is terminated in its characteristic impedance will act as a delay line for any input wave form. The delay time is $T = L/v$, L being the length of the cable. For an imperfect, but practical cable, that is terminated in a resistor with the characteristic impedance of the cable, the most usual source of error is a distributed leakage resistance between the

Physical Cable

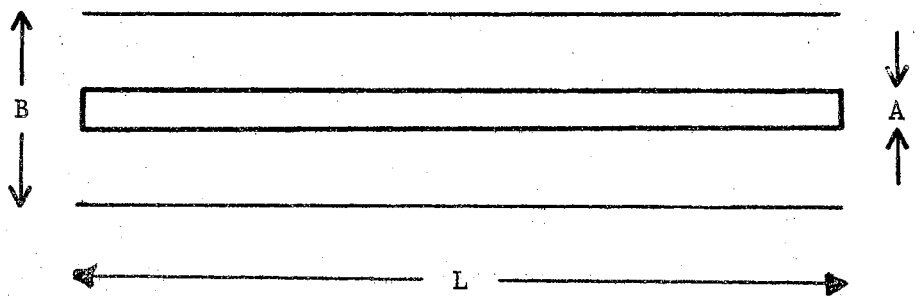

Electrical Equivalent

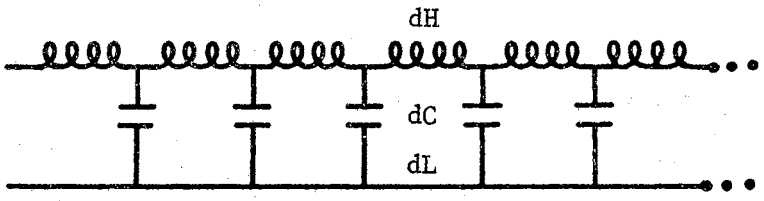

$H_L = dH/dL$

$C_L = dC/dL$

Electrical Symbol

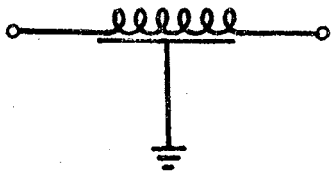

Figure 5. The Coaxial Cable

center conductor and the outer conductor, or shield. This leakage results in different frequencies propagating with different velocities. The second most common defect in practical cables is a failure for R_o to have the same value from one end of the cable to the other, including connectors. It is customary to refer to any length of coaxial cable as a delay line, even if it is not terminated in its characteristic impedance.

The parameters for a coaxial cable depend on the variable dimensions A and B, and on the dielectric constant, k. A list of these parameters and the equations which determine them are collected in Table II.

Reflections at the Termination of a Coaxial Cable

A wave form traveling along a finite-length, coaxial cable delay line will eventually reach the end of the cable. If the cable is not terminated by its characteristic impedance, the wave form will be reflected, and travel back toward the input terminals. The amount of the reflection will depend upon the value of the terminating resistance. In this section, reflection of a wave form at the termination of a coaxial cable will be discussed.

The general solution for the voltage, E, and current, I, along a coaxial cable delay line as a function of the distance along the cable, x, and the time, t, is given by

$$E(x,t) = F_1(t - x/v) + F_2(t + x/v)$$

$$I(x,t) = 1/R_o \cdot [F_1(t - x/v) - F_2(t + x/v)]$$

F_1 is an arbitrary function of $t - x/v$ and represents a wave traveling

TABLE II

COAXIAL CABLE PARAMETERS

Known Parameters	Universal Constants
A (Inside Diameter)	ε_o (Electric Permittivity of Free Space) $= 10^{-9}/35.952\ \pi$ fd/m
B (Outside Diameter)	μ_o (Magnetic Permeability of Free Space) $= 4\ \pi \times 10^{-7}$ hy/m
k (Dielectric Constant)	

Determinable Parameters

Capacitance per Unit Length	C_L	$= 2\ \pi\ k\ \varepsilon_o/\text{Ln}\ (B/A)$ fd/m
Inductance per Unit Length	L_L	$= (\mu_o/2\pi)\ \text{Ln}\ (B/A)$ hy/m
Characteristic Impedance	R_o	$= (1/2\ \pi)\sqrt{\mu_o/k\ \varepsilon_o}\ \text{Ln}\ (B/A)$ ohms
Velocity of Propagation	v	$= 1/\sqrt{k\ \varepsilon_o \mu_o}$ m/sec

in the direction of increasing x; F_2 is an arbitrary function of $t + x/v$ and represents a wave traveling in the opposite direction. The specific solution for wave propagation along a coaxial cable delay line is obtained by combining waves traveling in opposite directions in such a way that the boundary condition is satisfied at each termination. The requirement that E/I equal the terminating impedance is a statement of a boundary condition.

Consider an infinitely long delay line to which is applied the unit step voltage, U(t).

$$U(t) = 0 \; ; \; t < 0$$

$$U(t) = 1 \; ; \; t \geq 0$$

There is no reflected wave from the end of the cable, and the solution for the voltage and current is given by

$$E(x,t) = U(t - x/v)$$

$$I(x,t) = 1/R_o \cdot U(t - x/v)$$

Since $R_o = E/I$, an infinitely long, delay line acts as a resistance of value, R_o.

Assume that U(t) is applied to a delay line of finite length, L, which is terminated by R_o. It is observed that the boundary condition is satisfied by the solution that is given for the infinitely long delay line. It is concluded that a delay line which is terminated in its characteristic impedance does not reflect an incident wave.

For the case in which the terminal resistance, R, of a finite length delay line is not equal to R_o, the solution is quite different

from the two preceding cases. Assume that a unit step voltage is applied to a delay line of length, L. Then a voltage reflection coefficient, p, is found, which is defined by the following equations:

$$E(x,t) = U(t - x/v) + p \cdot U(t - 21/v + x/v)$$

$$I(x,t) = (1/R_o) [U(t - x/v) - p \cdot U(t - 21/v + x/v)] .$$

A current reflection coefficient, q, may be defined.

$$q = - p .$$

It may easily be shown that the voltage reflection coefficient is given by

$$p = \frac{R/R_o - 1}{R/R_o + 1} .$$

Two special cases are of particular interest. In the first case, R is equal to infinity (open-circuited line), for which, p = + 1 and q = - 1. For R = 0 (short-circuited line), p = - 1 and q = + 1.

The Coaxial Cable Pulse Generator

A length of coaxial cable will act as a pulse generator if it is charged to a voltage, V. It may be discharged through a load resistance, just as a capacitor would be discharged. The energy stored in such a pulse generator is given by the usual formula for capacitive energy storage, $W_c = \frac{1}{2} C V^2$, where $C = C_L L$ and L is the length of the pulse generator. The pulse generator that is constructed in this manner has characteristics different from those of a simple capacitor that is discharged through a resistor. The voltage rises as a step function, is

constant for a short period of time, and then falls to zero as a step function.

The operation of the coaxial cable pulse generator is explained by applying its Thevenin equivalent circuit. This circuit diagram and a schematic diagram for the pulse generator are shown in Figure 6. When the switch, S, is closed, the voltage drop across R is

$$E_R = \frac{R\,V}{R + R_o} \quad .$$

It is noted that there is a discontinuity in voltage at the load resistance, its amplitude being

$$E_R - V = - \frac{R_o\,V}{R + R_o} \quad .$$

Suppose $R = R_o$, then this discontinuity is of magnitude - V/2. This discontinuity travels down the cable and discharges it to a voltage, V/2. When this discontinuity reaches the open end of the cable, it is reflected without inversion, discharging the cable completely. It is thus concluded that a length of coaxial cable charged to a voltage, V, and discharged into a load resistance equal to the characteristic impedance of the cable, will produce a square voltage pulse of amplitude V/2 and duration 2T.

In the next section, the reflection of a square voltage pulse from the termination of a coaxial cable is considered. For this study it is desirable to have an analytic expression for such a wave form. Consider a square voltage pulse, $E_p(t)$, of amplitude V_o, and duration t_p. This pulse may be represented in terms of the unit step voltage.

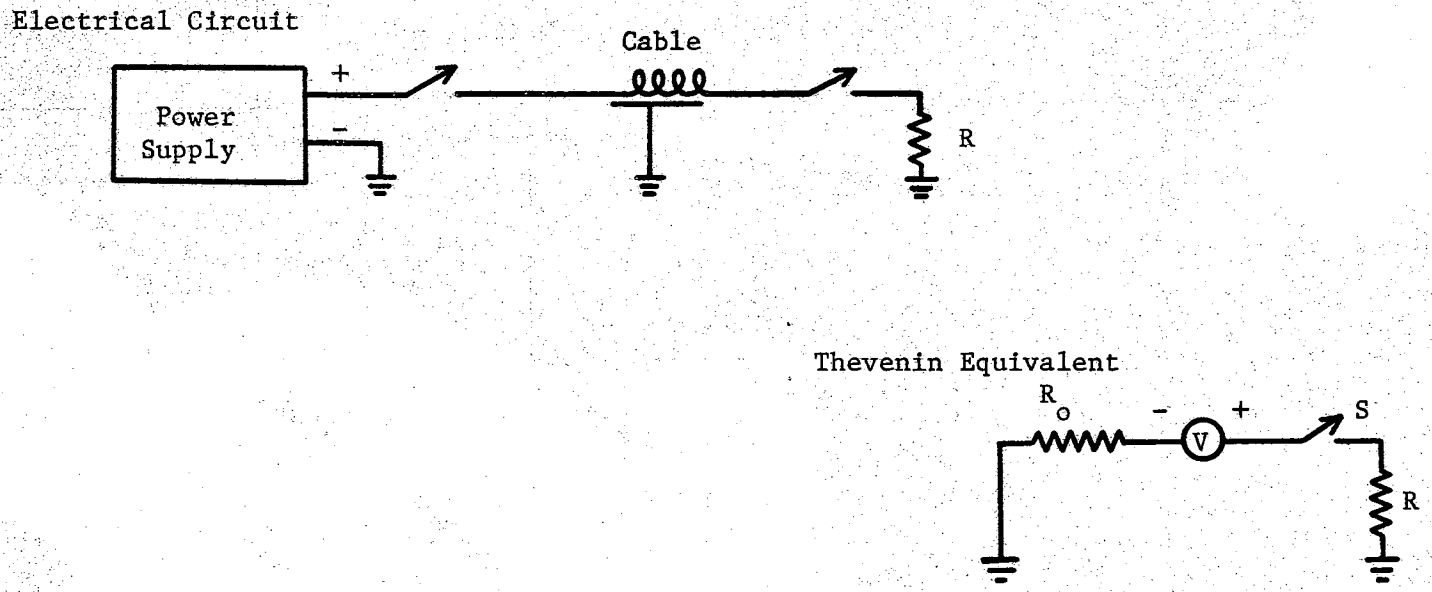

Figure 6. The Coaxial Cable Pulse Generator

$$E_p(t) = V_o [U(t) - U(t - t_p)] ,$$

where the boundary conditions are

$$E_p = 0 \; ; \quad t < 0$$

$$= V_o \; ; \; 0 \leq t < t_p$$

$$= 0 \; ; \quad t \geq t_p$$

The Coaxial Cable Circuit for Exploding Wires

In the preceding three sections of this chapter the basic concepts for constructing a coaxial, "exploding wire" system were considered. In this section, these concepts will be assembled and relevant equations presented.

Essentially, the "exploding wire" circuit consists of a pulse generator, a delay line, and the wire to be exploded as illustrated in Figure 7. The pulse generator is charged to a voltage, V, and discharged into the delay line. Since the characteristic impedance of the delay line is the same as that of the pulse generator, a square voltage pulse will be launched down the delay line. The wire forms a resistive termination for the delay line. When the pulse arrives at the wire, current passes through it, and causes its resistance to change. The voltage reflection coefficient at this termination is, consequently, time dependent.

$$p = p(t) = \frac{R(t)/R_o - 1}{R(t)/R_o + 1}$$

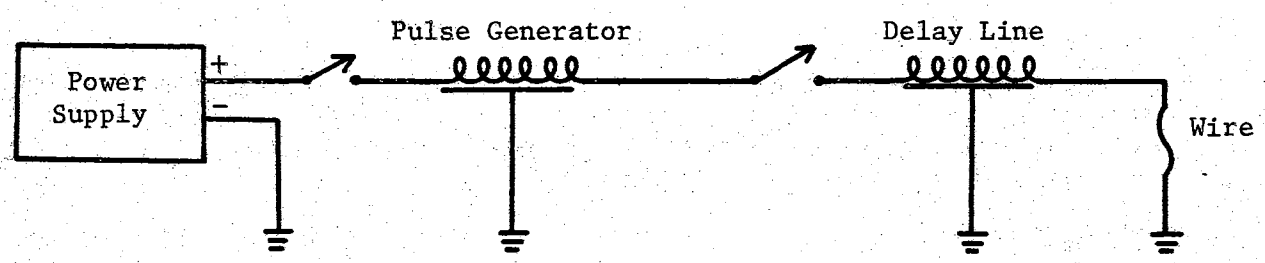

Figure 7. Basic "Exploding Wire" Circuit

The next problem is to determine the reflection of a square voltage pulse at a time dependent resistive termination of a coaxial cable.

For the situation described in the preceding paragraph, the current and voltage along the delay line are represented by the following equations.

$$E(x,t) = E_p(t - x/v) + p \cdot E_p(t - 2L/v + x/v)$$

$$I(x,t) = 1/R_o \cdot [E_p(t - x/v) - p \cdot E_p(t - 2L/v + x/v)] .$$

The primary concern is the voltage and current at the wire termination, that is, at $x = L$. Making the substitution for $U(t)$, the following relations are obtained:

$$E(L,t) = V_o (1 + p) [U(t - L/v) - U(t - L/v - t_p)]$$

$$I(L,t) = (V_o/R_o)(1 - p) [U(t - L/v) - U(t - L/v - t_p)] .$$

For times such that $t < L/v$, the pulse has not yet arrived at the wire termination; consequently, $E(L,t) = I(L,t) = 0$. It is, therefore, convenient to define a new time variable, t', such that the pulse is just arriving at the wire termination at $t' = 0$. This requires the substitution $t' = t - L/v$, to give

$$E(L,t') = V_o (1 + p) [U(t') - U(t' - t_p)]$$

$$I(L,t') = (V_o/R_o) (1 - p) [U(t') - U(t' - t_p)] .$$

The only times during which voltage appears across the wire and energy is inserted are times for which $0 \leq t' \leq t_p$. For such times,

$$E(L,t') = V_o (1 + p),$$

$$I(L,t') = (V_o/R_o)\,(1 - p) .$$

Substituting for p(t'), the following is obtained after some algebraic manipulations.

$$Y(t') = 2G(t')/(1 + G(t'))$$

$$K(t') = 2/(1 + G(t')),$$

where

$$Y(t') = E(L,t')/V_o$$

$$G(t') = R(t')/R_o$$

$$K(t') = I(L,t')/I_o \; ; \; I_o = V_o/R_o$$

Since there are two equations in three variables, one of them must be considered as independent. It seems most convenient to let Y(t') be the independent variable, since it is the voltage that is most readily measured on the oscilloscope. Considering Y(t') as the independent variable, the following is obtained.

$$K(t') = 2 - Y(t')$$

$$G(t') = Y(t')/(2 - Y(t'))$$

Consideration is now given to the input of energy to the wire by means of joule heating. The rate of energy input to the wire is given by

$$\dot{W}(t') = I(L,t')\,E(L,t')$$

The total energy input is obtained by integrating $\dot{W}$ over the time inter-

val of the square voltage pulse. Thus,

$$W = P_o \int_0^{t_p} Y(t') \, (2 - Y(t')) \, dt' ,$$

where

$$P_o = I_o V_o$$

The energy content of the wire at any other time, t, between 0 and t_p is determined by integrating between the limits 0 and t.

Cable Circuits for Increasing Energy

It is desirable that there be a means of increasing the energy delivered to the wire to be exploded, without increasing the length of the voltage pulse in which the energy is contained, and without increasing the voltage to which the pulse generator is charged. Increasing the voltage beyond a certain point becomes impractical, because dielectric breakdown begins to occur. The problem is one of designing a pulse generator using several lengths of cable, in such a way that the characteristic impedance of the generator matches that of the delay line into which it is discharged.

The general scheme for accomplishing the above is as follows. Select n^2 sections of cable of length, L (n, a positive integer). These n^2 cables are divided into n groups of n cables each. All the cables of each group are connected in parallel and charged to a voltage, V. In each case the center conductors are charged to the higher voltage. All the n groups are then connected in series. When this arrangement

is discharged, a voltage pulse of amplitude, n V, is produced. The length of the pulse is exactly the same as would be produced by a single cable of length, L. This means that the energy of the pulse has been increased by the factor, n^2.

An illustration of a pulse generator using four cables appears in Figure 8. This figure illustrates how the cables are connected after they have been charged to the appropriate voltage.

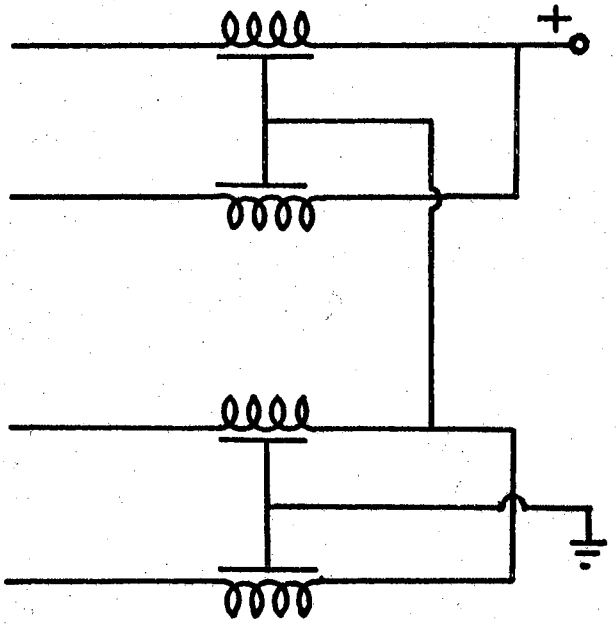

Figure 8. Four-Cable Pulse Generator

CHAPTER IV

COMMENTS ON SPARK GAP BREAKDOWN

As indicated in Chapter I, three different spark gaps are employed in the coaxial cable "exploding wire" system. One gap starts the pulse down the coaxial cable delay line. A second gap sharpens the leading edge of the pulse before it impinges upon the wire. The third gap is a three-electrode gap and is employed to divert the reflected pulse into a dissipative circuit that absorbs the energy in the pulse without reflections.

Basically, a spark gap consists of two, separated, metal electrodes emerced in a confined gas. Application of a sufficiently high potential difference across the electrodes results in a breakdown with the flow of a large current. Breakdown occurs when a sufficient potential difference is applied and held long enough to cause the dynamic resistance of the space between the electrodes to approach very near to zero. A study of spark gaps, thus, becomes one of the phenomena of electrical breakdown of gases. The literature on this subject is very extensive. Any elaboration of details would be out of place here. Rather, an overview of the subject is presented in order to place the understanding of spark gaps in proper perspective to the purpose of this thesis.

Factors Affecting Spark Gap Breakdown

The factors which affect spark down breakdown can be classified as

either external or internal. There are many external factors which affect spark gap breakdown, the most prominant of which are:

1. Gas in the gap
2. Initial temperature and pressure of the gas
3. Ambient radiation present
4. Impedance and nature of the voltage source
5. Electrode spacing and shape
6. Rate of rise of the voltage across the gap
7. Electrode composition, state of oxidation, etc.

In contrast to the above mentioned external factors, there are internal mechanisms of breakdown which occur in the gas. In the literature, these have been divided into two groups:

1. The primary ionization process
2. Secondary ionization processes

The process of primary ionization (α effect) occurs when electrons crossing the gap collide with atoms, producing ion pairs. Theoretically, this process cannot cause breakdown by itself. For breakdown to occur, the current must increase without bound, limited only by the source supplying the voltage. In order to explain breakdown, secondary ionization processes have to be introduced. A number of secondary processes have been recognized to contribute to breakdown in gases. The magnitude of each effect varies with the external factors, especially with the pressure of the gas. In the literature, two main approaches have been advanced to explain breakdown, the Townsend avalanche theory, and the streamer theory (Meek and Craggs, 1953). The Townsend theory is a low pressure theory including ionization at the electrode surfaces. The basic secondary processes contributing to the Townsend theory are

the β, γ, δ, and ϵ processes, which are briefly described as follows:

1. β effect: Ionization of the gas by positive ions created by the passage of an initial electron.
2. γ effect: Emission of secondary electrons by the cathode under impact by positive ions in the discharge.
3. δ effect: Emission of secondary electrons by the cathode under impact by photons coming from the discharge.
4. ϵ effect: Emission of secondary electrons by the cathode under impact from excited atoms in a metastable state.

The Streamer theory is a high pressure theory which ignores ionization at the electrodes. This theory is controlled by the η and σ effects given below:

1. η effect: Photo-ionization of the gas. This process becomes significant at high pressures. Impurities in the gas tend to decrease, or even to block this effect.
2. σ effect: Effect of Space Charge. When the applied pressure or potential difference is very high, the density of charges of each sign rapidly assumes a value such that the electric field is strongly perturbed. Beyond a critical threshold, it becomes possible for ionization of the space between the charges to rise sharply.

The present state of the art is one in which there is controversy over the role played by the various processes at different pressures. This is evidenced by a recent journal article describing production of streamers at low potential gradients (Acker and Penney, 1969).

Paschen's Law

Of great practical importance is a knowledge of the relation between the gas pressure, electrode spacing, and breakdown voltage for a particular spark gap arrangement. A relation which is valid for a limited range of parameters is known as Paschen's law. Although it is an experimental law, it does have some theoretical justification from a combination of the Townsend theory with some elementary kenetic theory.

Let P be the gas pressure, d, the electrode separation, and V_b, the breakdown voltage. Then, Paschen's law is stated in two parts:

1. V_b is a unique function of the product, P d.
2. V_b has a minimum in the range of low P d.

A curve which expresses Paschen's law is known as a Paschen's curve. Its general form is illustrated in Figure 9.

Experimental evidence indicates that Paschen's law is valid in the approximate region, $0.01 < P\ d < 20$, where P d is measured in units of cm x psi (Papoular, 1965). Breakdown phenomena in the low P d range are of no concern to the purposes of this thesis, but values of P d up to approximately 50 are required to hold off the high potential differences to which the pulse generator is charged. When the pressure becomes high enough, V_b is no longer a unique function of P d. In this region, a relation, that was established by experiment and was later justified by means of the streamer theory, is known as Raether's criterion for breakdown. This criterion seems to give results consistent to within about 10 percent of experimental values. It is expressed by the following equation:

$$(\alpha d)_c \simeq 20,$$

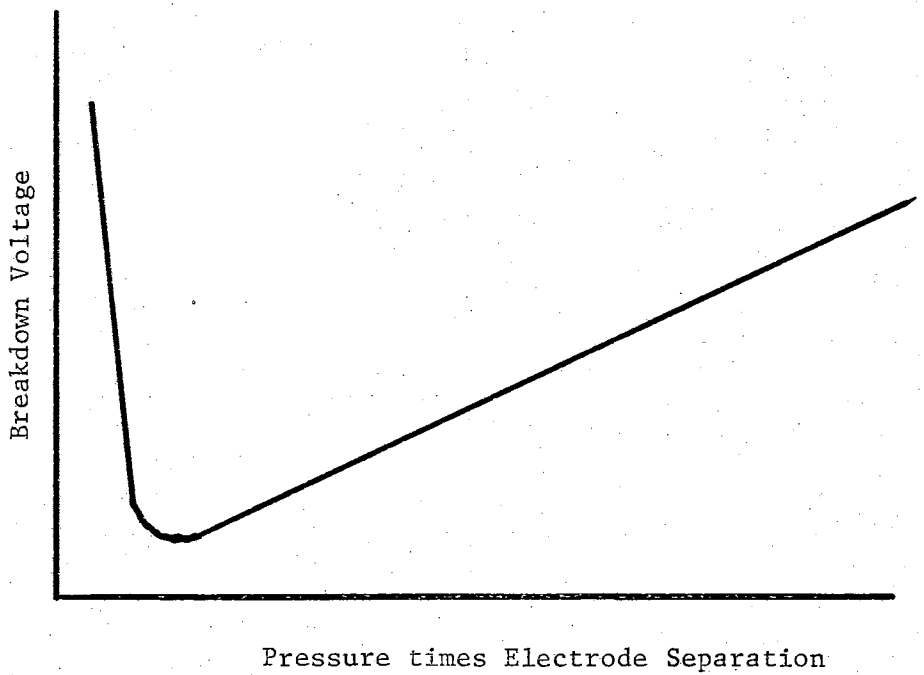

Figure 9. Paschen's Curve

where α is the number of ion pairs that are produced per unit length of electron travel. The subscript, c, denotes that α corresponds to a critical charge density which appears in the theory. In the next chapter, an experimental Paschen's curve for nitrogen is extended to the high P d region by using Raether's criterion.

Time Lag

When the voltage on a spark gap is increased very, very slowly, the voltage at which the gap breaks down is called the dc (direct current) breakdown voltage, V_{dc}. When the voltage is applied more and more rapidly, the voltage at which breakdown occurs, V_{bd}, becomes larger and larger. The difference between these voltages is called the overvoltage, V_{ov}, and the following relation exists.

$$V_{bd} - V_{dc} = V_{ov} > 0$$

For a pulse of voltage with a very rapid rise at the front of the pulse, the overvoltage may be large; that is, it may be larger than V_{dc}.

With a steeply rising voltage, there is a lag between the time that the steep front reaches V_{dc} and the breakdown occurs at V_{bd}. This time lag depends on the amount of overvoltage, the pressure of the gas about the gap, the electrode separation, the electrode shape and surface effects on the electrodes which are usually called the Paetow effects. The time lag is important for the design of the pulse shaping gap. The time lag decreases with an increase of overvoltage, and with very large overvoltages, time lags may be as small as tens of nanoseconds, or less. Below 0.05 per cent overvoltage, time lags may be of the order of milliseconds. An increase of the electrode spacing increases the amount of

time lag. The time lag increases with an increase of pressure, with some restrictions. The pressure must be in excess of a critical pressure, and the amount of overvoltage must be constant.

Switching Action

As discussed in the preceeding portion of this chapter, a two-electrode spark will hold off voltages up to a critical breakdown voltage. For purposes of switching, the problem becomes one of changing from a very good insulator at less than breakdown voltage, to a conductor. Williams (1959) lists eight ways to accomplish this:

1. Increase the voltage across the electrodes.
2. Reduce the electrode spacing.
3. Reduce the gas density (pressure).
4. Irradiate the gap with radioactive materials, or x-rays.
5. Ultraviolet irradiation of the gap.
6. Emission of electrons from a hot filament in the gas.
7. Injection of electrons and/or electrons into the gap.
8. Distortion of the electric field.

The Switching Gap

After the pulse generator is charge to a voltage, V, it must be discharged into the delay line to produce a square voltage pulse. This is accomplished by "firing" the switching gap which is illustrated in Figure 1. The gap housing is filled with gas to a high pressure such that breakdown cannot occur. A valve is opened which allows the gas to exhaust from the gap housing. The gas pressure between the electrodes eventually becomes low enough for breakdown to occur.

Pulse Shaping Gap

As the square voltage pulse travels along the delay line toward the wire to be exploded, it loses some of its high frequency components on account of the imperfect nature of the delay line. This loss considerably extends, that is, increases, the rise time of the voltage pulse at the wire. This would result in inaccurate calculations from the oscillographic traces. To Obtain a more rapid rise of voltage, a second spark gap is inserted at the end of the delay line, just ahead of the wire. This gap has a shorter electrode spacing than the switching gap and is overvolted by the pulse. In accordance with Fletcher (1949), the operation of the pulse shaping gap is explained as follows. The pulse generator is discharged into the delay line. When the pulse arrives at the pulse shaping gap, this gap has a large overvoltage on it and breaks down very rapidly after its normal lag time. If this lag time is longer than the rise time for the voltage on the switching gap, the pulse appearing on the other side of the pulse shaping gap is determined by the second gap, rather than the first. This cause a pulse sharpening effect

The Triggered Gap

As stated earlier, it is desirable for the plasma from the exploded wire to expand in a field free region. If the pulse that is reflected from the wire is not eliminated, it will eventually be reflected back into the wire. This would apply a field during the expansion of the plasma. To eliminate this reflected wave, a triggered spark gap is "fired". This diverts the wave and discharges its energy into a resistor. This resistor terminates a length of coaxial cable and is mounted

as part of the center conductor. The value of the resistor is equal to the characteristic impedance of the cable; in this way, there is no reflection from this termination.

The triggered spark gap is connected in a "T" fashion on the wire side of the switching gap, as is illustrated in Figure 1. A small portion of the original square voltage pulse is diverted to a time delay. After appropriate delay, the output of the delay activates a thyratron circuit which "fires" the triggered gap.

The triggered gap must be able to hold off the initial square voltage pulse and must be capable of being "fired" to within an accuracy of perhaps 1/10 of a microsecond. A method which appeared capable of accomplishing this is the three-electrode spark gap. Two basically different types of three-electrode gaps are illustrated in Figure 10. Each types consists of two main electrodes, across which breakdown occurs, and a trigger electrode which "fires" the spark gap. Type I has the trigger electrode mounted coaxially within one of the main electrodes, and is insulated from it. In type II, the trigger electrode is mounted separately from the two main electrodes and at right angles to them. At "firing" time, a voltage is place across electrode B and the trigger electrode, causing breakdown. The three-electrode gap of type II seemed best suited to the present application for the following reasons:

1. With type II, all three electrodes may be made adjustable.
2. Type II allows for variation of the trigger electrode geometry.
3. Fabrication of type I becomes difficult since both of the main electrodes are connected as the center conductor of a coaxial cable.

Type I

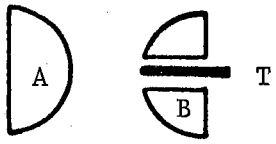

Type II

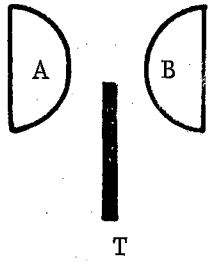

A, B ... Main Electrodes

T .... Trigger Electrode

Figure 10. Three-electrode Spark Gap Types

CHAPTER V

SYSTEM HARDWARE

In the preceeding chapters, the theory relating to the "exploding wire" system was discussed. In this chapter, the electrical circuitry is discussed in greater detail, and the design features of the various machined parts are presented. A block diagram of the complete system is shown in Figure 11. This diagram serves as a basis for the present discussion.

The Power Supply

In order to obtain a high input current to the wire, it is necessary to charge the pulse generator to a high voltage. The power supply to accomplish this is the Keleket 115,000 volt, x-ray transformer, which is modified as illustrated in Figure 12. Primarily for safety reasons, the case of the high voltage transformer is raised above ground, the center tap of the secondary winding is left ungrounded, and the negative output terminal is grounded. The primary of the high voltage winding and the primaries of the filament windings are isolated by means of 1:1 isolation transformers which were constructed for this purpose. The control box which is illustrated in Figure 12 consists, mainly, of an auto-transformer. With the auto-transformer, the output voltage of the high voltage transformer may be increased in steps of approximately 1000 volts The primary of the auto-transformer is connected to a 220

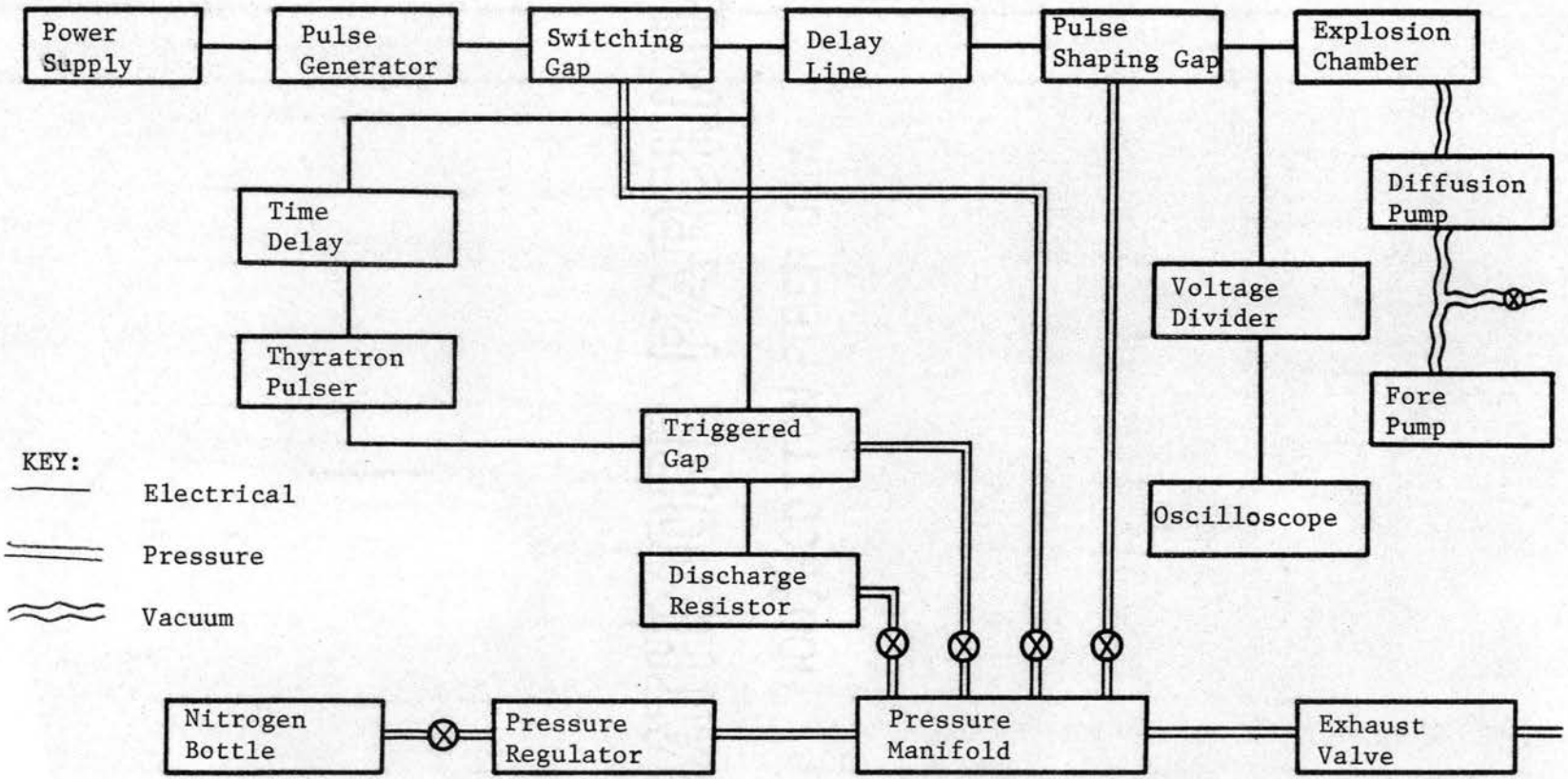

Figure 11. Block Diagram of "Exploding Wire" System

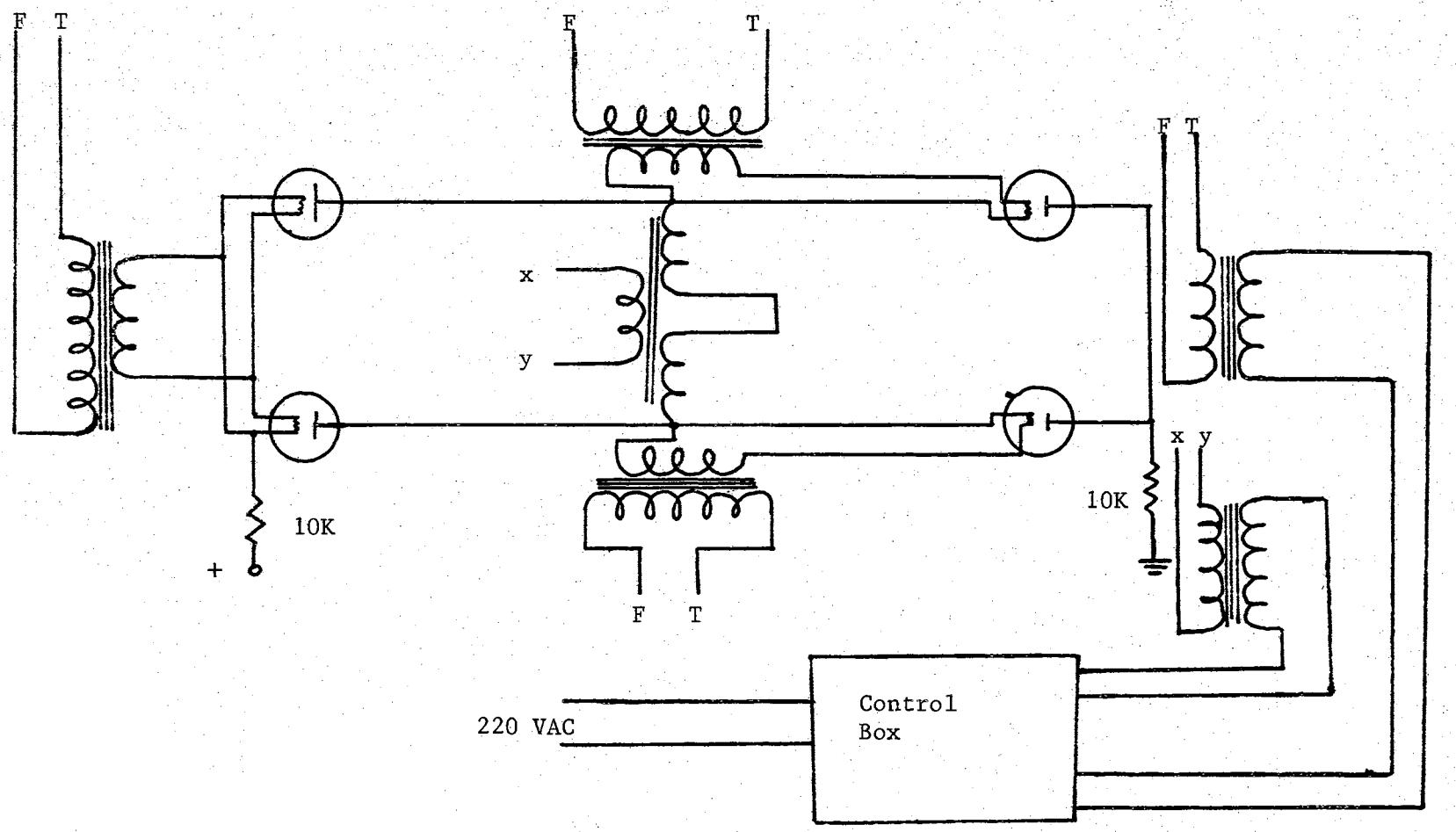

Figure 12. High Voltage Power Transformer

volt A. C. line. If the pulse generator is charged to the full 115,000 volts, then the initial current in the wire is approximately 2300 amperes.

A small inductor is placed in series with the positive output terminal of the power supply. This is to prevent surge currents, which might be produced in the pulse generator, from damaging the power supply. A surge current, which is incident upon the positive terminal of the power supply, is reflected by the inductor.

In order to allow the pulse generator voltage to build up gradually, a 25 megohm resistance is placed in series with the inductor and the pulse generator. This resistance consists of 25, 1 megohm resistors connected in series and mounted in a section of phenolic tubing, as illustrated in Figure 13. By using resistors which are rated at 2 watts, 50 watts may be continuously dissipated. This means that approximately 35,000 volts may be placed across the charging resistance, and that the pulse generator can be charged in steps of any value, up to this value.

Between the inductor and the charging resistance is placed a knife switch. When this switch is closed, the pulse generator is charged, and the switch may be opened, remotely, by a cord. If this switch were not opened, energy would be continuously fed into the cable system after the "firing" of the switching gap.

The Cable Elements

The cable which forms the pulse generator and the delay line of the "exploding wire" system is RG-19A/U coaxial cable. The various paramaters for this cable are given in Appendix C.

The pulse generator consists of approximately 325 feet of the

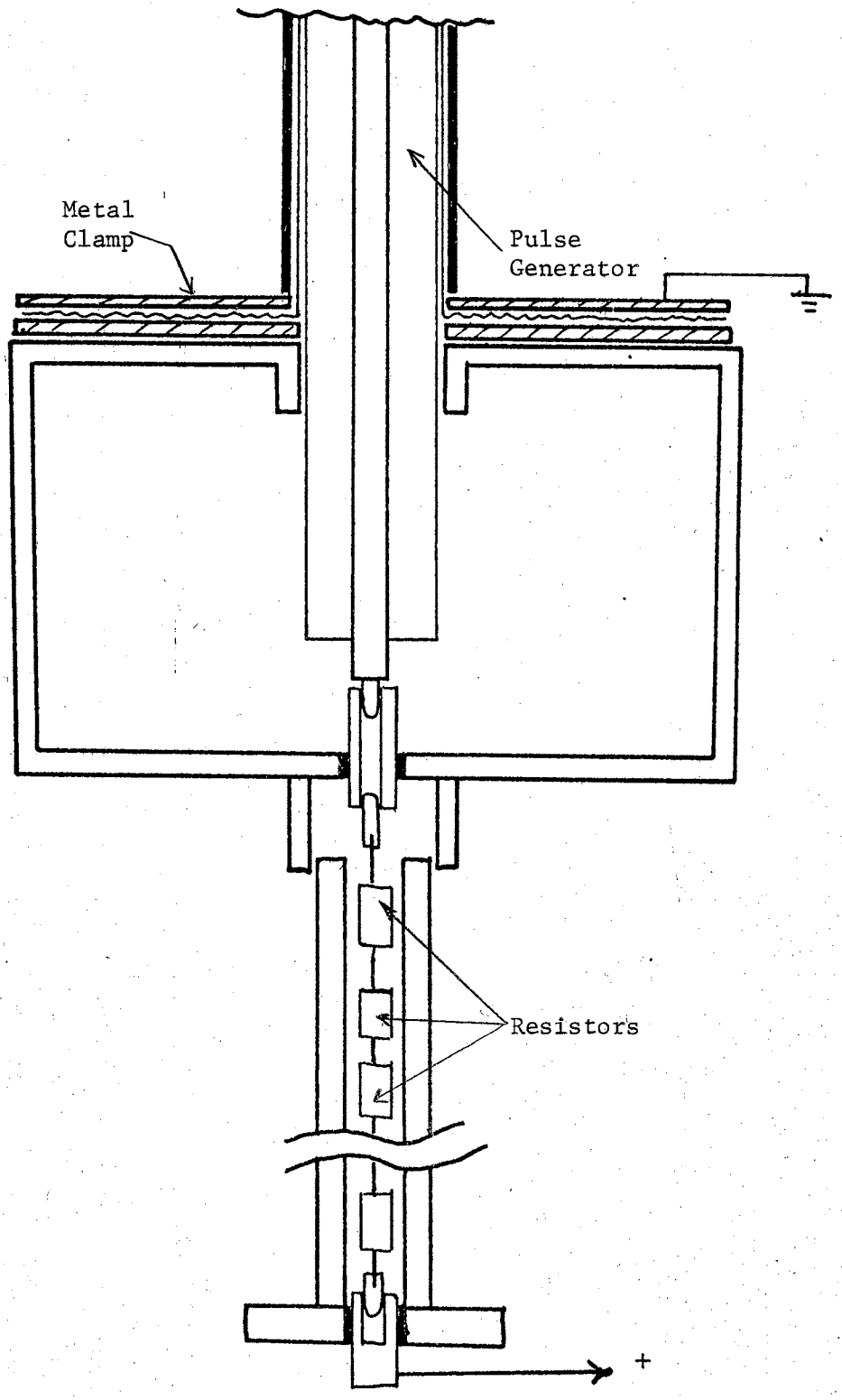

Figure 13. Charging Resistor Assembly

RG-19A/U cable. This length gives a pulse of approximately 1 microsecond. The distributed capacitance of the generator is approximately 10,000 pf. The value of the RC time constant of the charging resistance-generator combination is approximately 0.25 seconds. This means that the generator is able to charge to 98 per cent of full voltage in about 1 second.

The delay line consists of approximately 1675 feet of RG-19A/U cable. The two way delay time is approximately 5.7 microseconds. This long length of cable is desirable for two reasons:

1. The pulse generator must be discharged into its characteristic impedance. If the delay line is too short, the pulse generator will see the resistance of the wire rather than that of the delay line.
2. It is desirable for the delay line to be long enough so that the ionization in the switching gap is sufficiently reduced to withstand some of the reflected pulse before it breaks down. The pulse of reflected energy is diverted through the triggered gap rather than through the switching gap.

At various placed along the delay line, "T" connections are made as indicated in the electrical diagrams. The Amphenol #28000 "T" connector is employed. Since the required, coaxial connectors were not available, special connectors were fabricated to connect the cable to the "T" and to connect the "T" to external circuitry. The "T" and these connectors are illustrated in Figure 14. The main body of the connectors are made of brass. The insulating material is high density polyethelene.

The delay line is wound around the sides of an oval-shaped "cage", about 10 feet long, 4 feet wide, and six feet high. The pulse generator

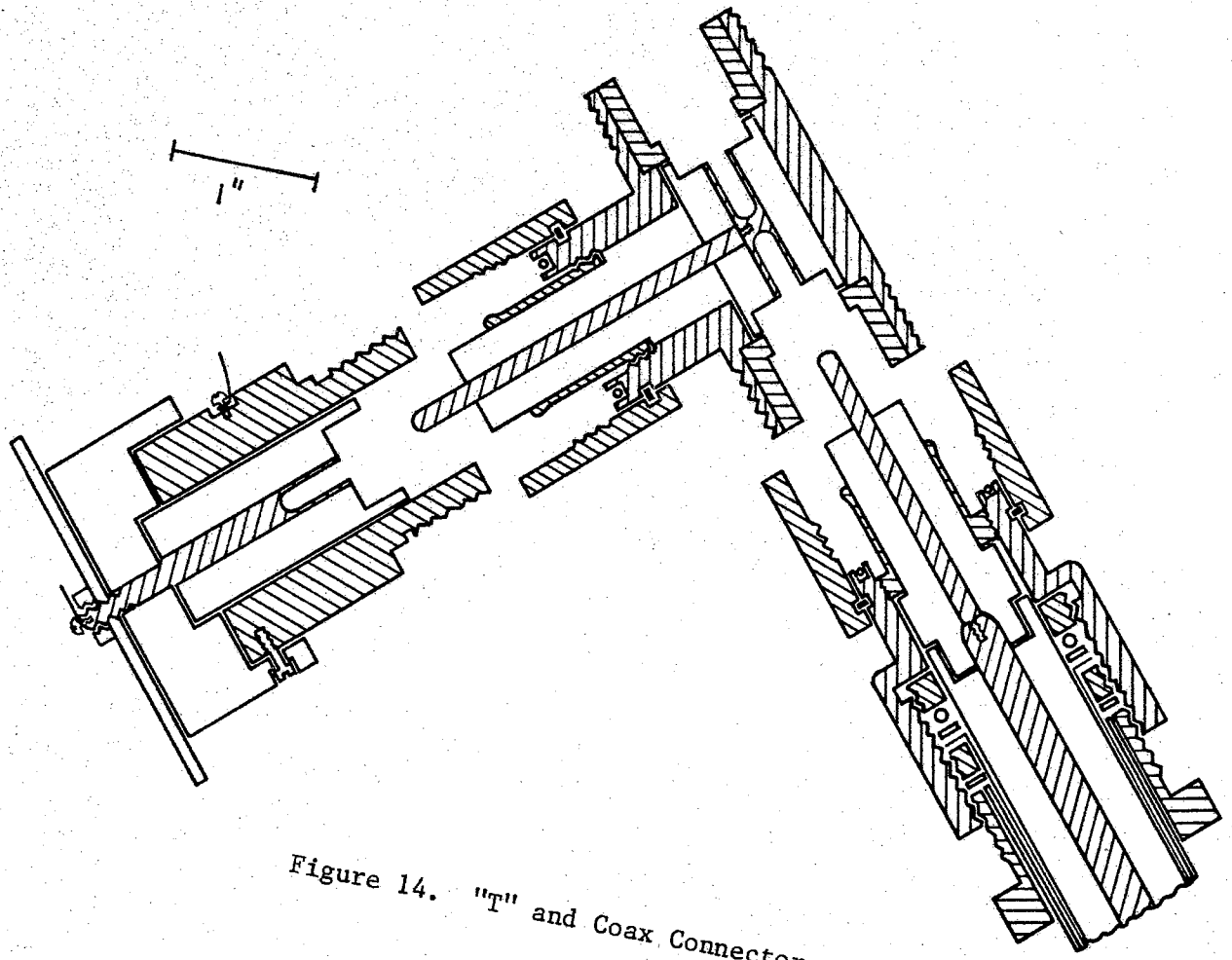

Figure 14. "T" and Coax Connectors

is mounted atop the "cage" on a spool about 4 feet in diameter.

The Spark Gaps

As discussed earlier in this thesis, there are three spark gaps in the "exploding wire" system: the switching gap, the pulse shaping gap, and the triggered gap. The first two of these are constructed in exactly the same manner and are illustrated in Figures 15 and 16.

In order to prevent the possibility of breakdown between an electrode and its housing, the dimentions of the housing, the insulating material, and the center conductor are tapered to a larger size. This taper is such that the ratio of the center conductor diameter to the housing diameter remains constant. In this way, the spark gap retains the characteristic impedance of the cable to which it is attached. This taper also prevents sharp voltage gradients which would result from abrupt changes of diameter.

A "donut" is placed between the two housings. This "donut" provides proper separation between the electrodes and provides an orfice through which nitrogen may be admitted. This assembly is held together by eight cap screws; pressure seals are made by standard industrial "O" rings.

All parts of the spark gap are made of cold rolled brass, except the hemispherical electrodes and the insulators. All current conducting, internal, metal parts are plated with a thickness of 0.002 inches of silver. This takes advantage of the high conductivity of silver to reduce the resistance of the conducting surfaces, which results from the "skin effect".

The insulators in the spark gap are made of high density

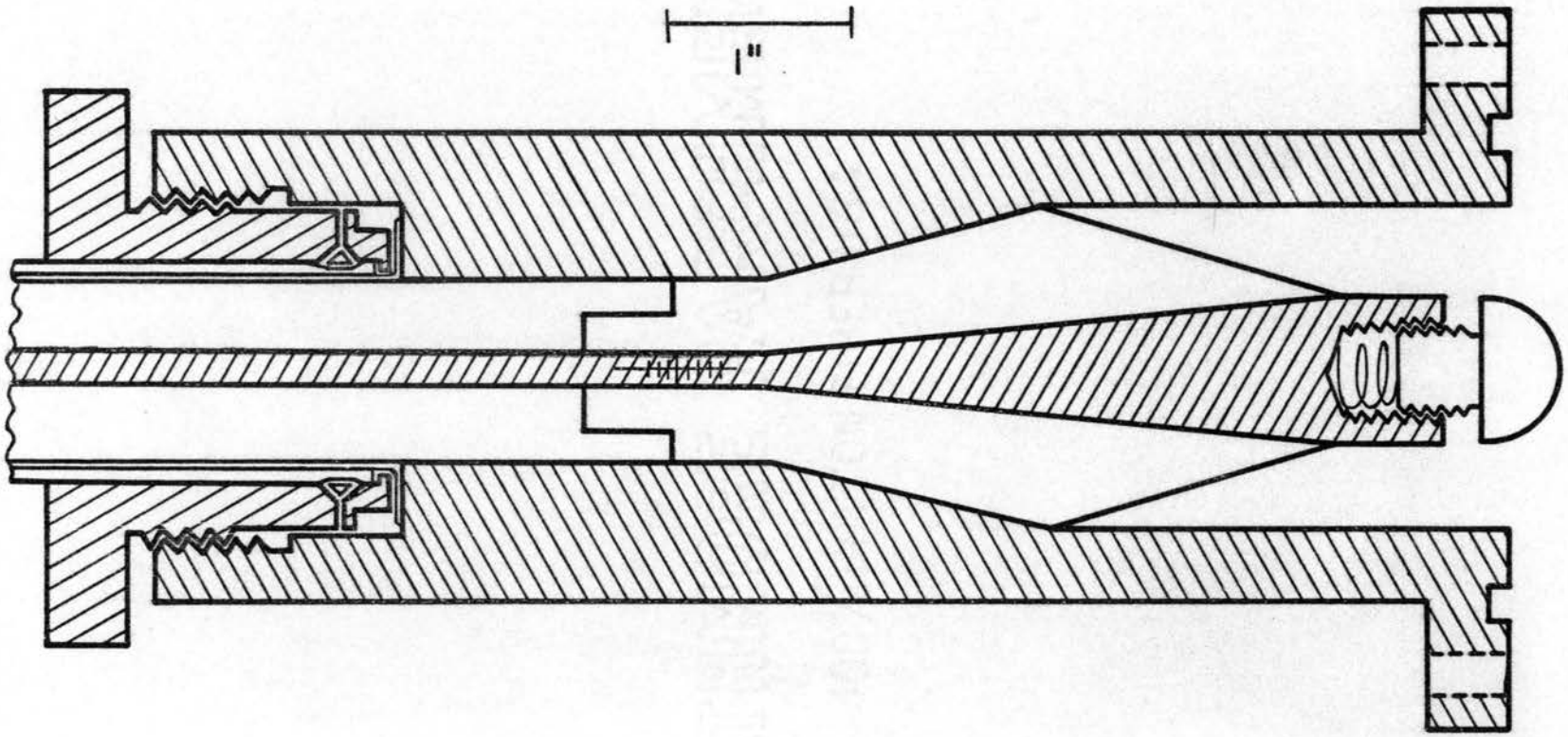

Figure 15. Spark Gap Electrode and Housing

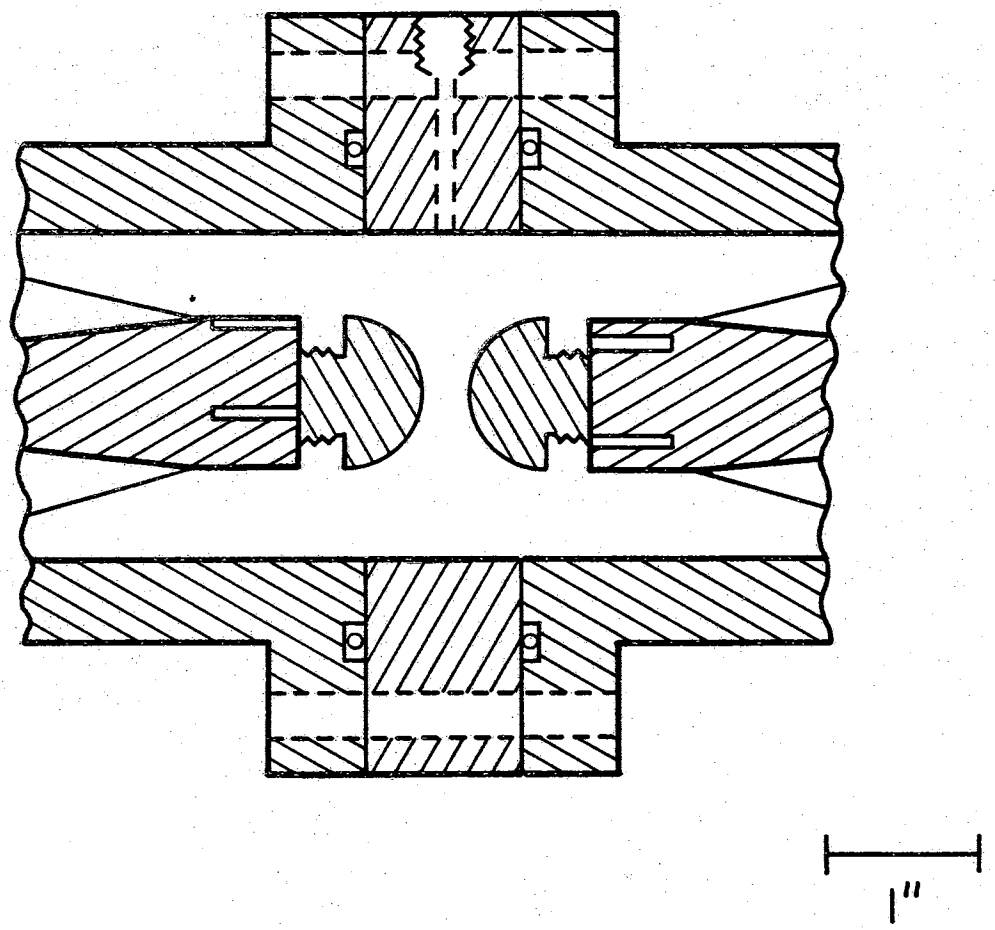

Figure 16. Assembled Spark Gap

polyethelene. Before insertion into the spark gap, the insulators are are coated with Dow Corning Compound 4. This compound is a non-melting, silicone dielectric and lubricant, which excludes moisture. It complies with the specification, MIL-I-8660. As a lubricant, it allows the insertion of the insulator into the housing to be accomplished with ease. As a dielectric, it fills the irregularities on the surface of the inlator, reducing the possibility of electrical leakage paths.

The two electrodes of the spark gap are hemispherical and are made of copper. Then they are plated with silver. They are screwed into the ends of the center conductors. Springs behind the electrodes maintain proper tension, and slots around the circumference of the ends of the center conductors prevent binding. This arrangement allows the separation of the two electrodes to be adjusted to appropriate values. The plane, parallel, and infinite electrodes, which are used for theoretical calculations, are impractical; therefore, the hemispherical electrodes are used. This design results in a slight decrease in the breakdown voltage. Peak (1929) predicts that the voltage gradient at the electrodes is increased by the factor,

$$f = d/4r + 1/4 + \sqrt{(d/4r + 1/4)^2 + 1/2}\ ,$$

where

d = electrode separation

r = electrode radius.

The maximum value of d/r is about 1/3 for these spark gaps. This gives gives a maximum value for f.

$$f_{max} = 1.115$$

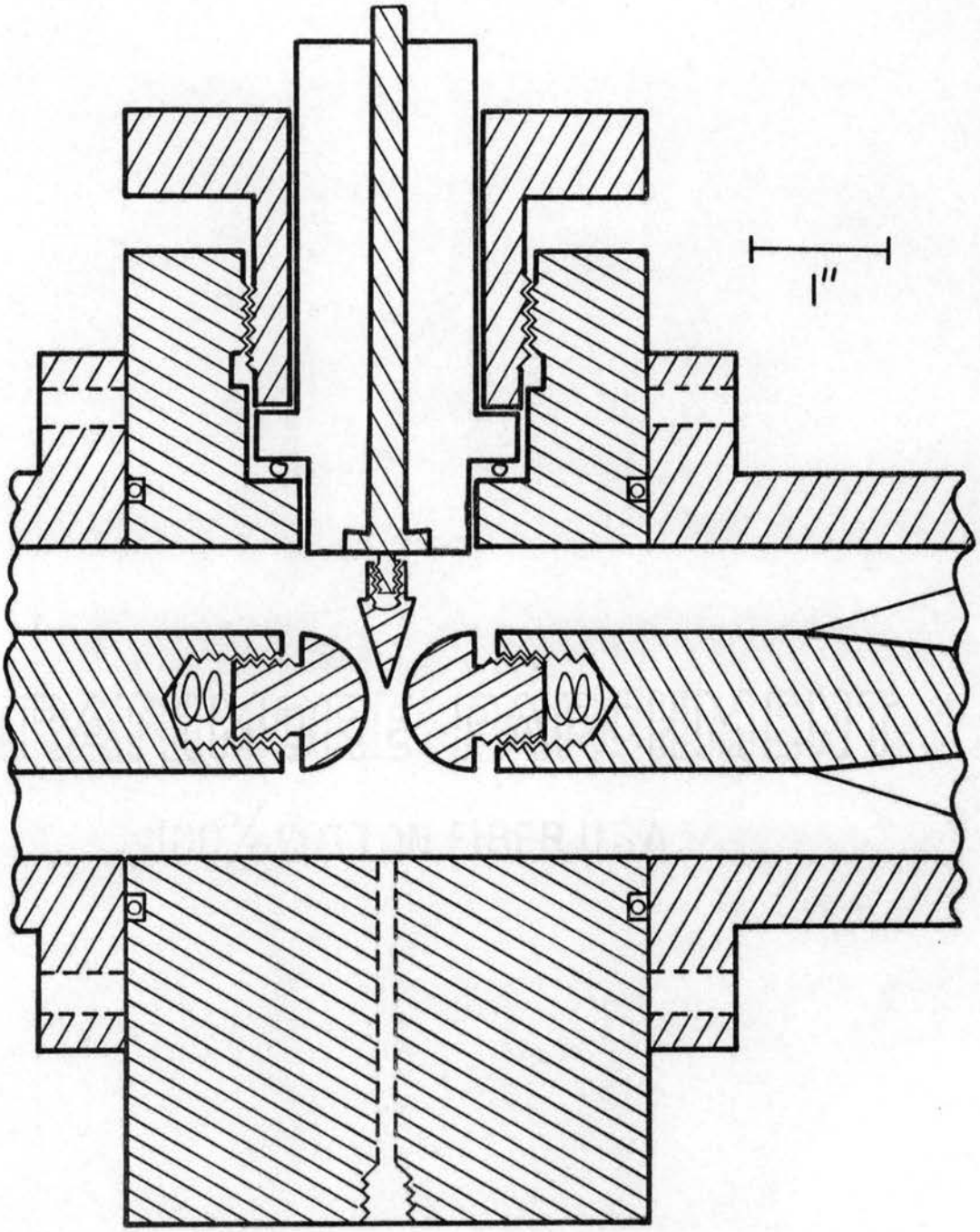

Figure 17. Triggered Spark Gap

The triggered spark gap is constructed in a manner which is very similar to the other two spark gaps. This gap is illustrated in Figure 17. The two main electrodes are constructed in exactly the same manner as for the other two spark gaps. The center conductors are somewhat extended and are made in two sections. In place of the "donut" of the first two gaps, there is an arrangement to house the trigger electrode. This electrode is made of copper, and is screwed onto the end of a stem which passes through a high density polyethelene insulator. This insulator is pressure sealed by an "O" ring and by a flange which has one side slightly tapered, on the end of the stem. A small orfice through the side of this arrangement allows nitrogen to enter the system.

The Discharge Resistor

After the reflected pulse from the "exploding wire" is diverted through the "fired", triggered spark gap, the pulse continues into a dissipation chamber where a 50-ohm resistor is mounted. This 50-ohm resistor matches the characteristic, or surge, impedance of the coaxial cable. Provided there is no mismatch of the surge impedance in the coaxial conductor between the triggered spark gap and the resistor, the energy is completely dissipated with no reflections. The resistor is mounted coaxially as is illustrated in Figure 18. The resistor is a Corning, H-type, and is non-inductive. The upper part of the housing is exactly the same as the housings for the spark gaps. The resistor is held by two holders which are slotted around the circumference. The bottom of the resistor housing is removable. This arrangement allows the resistor to be inserted or removed with ease.

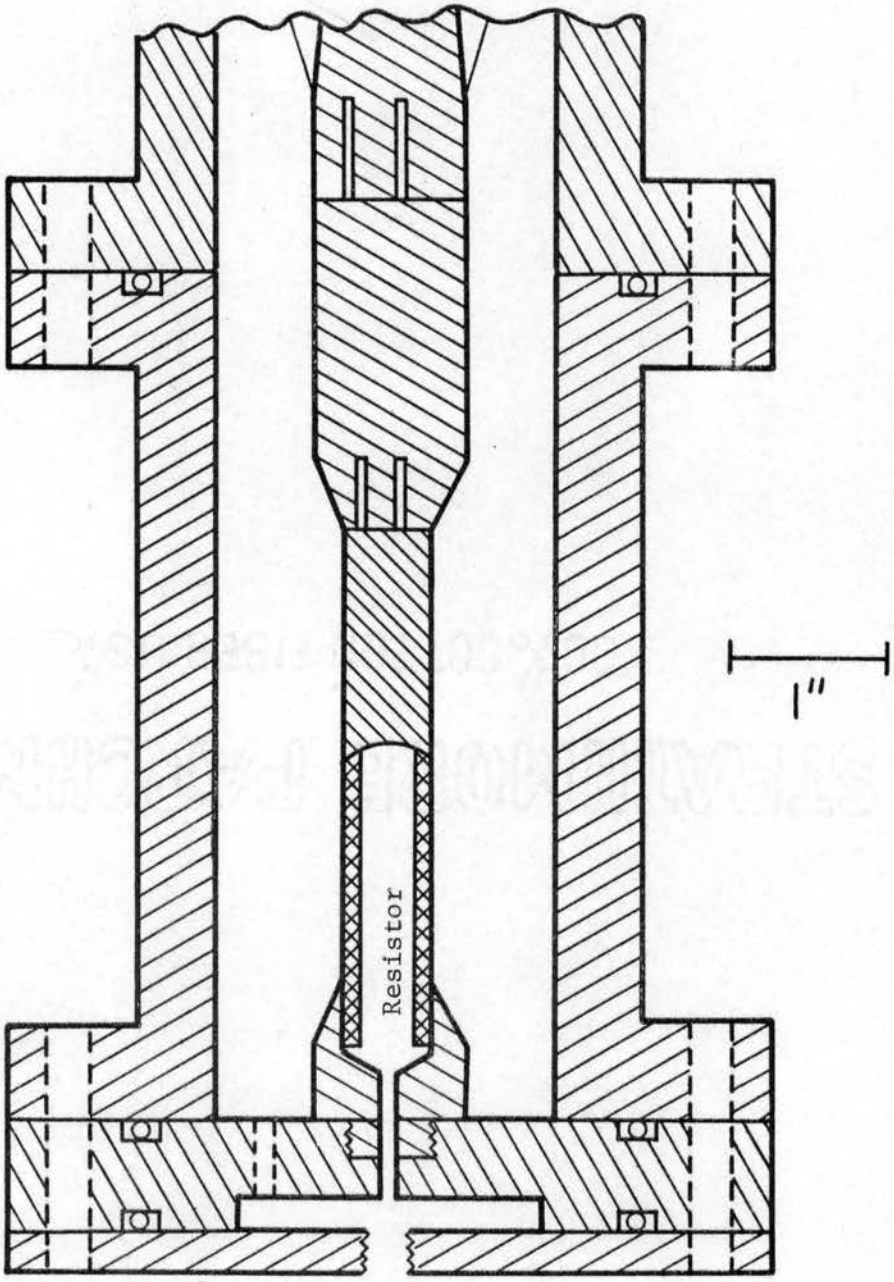

Figure 18. Coaxial Discharge Resistor

Electronic Circuitry for the Triggered Gap

The electronic circuitry, which is required to "fire" the triggered gap at the proper time, is shown in Figures 19 and 20. A signal from the delay line is fed through a voltage divider and an impedance matching network to a variable time delay. This delay is the AD-YU, type 553e, variable from 0 to 15 microseconds. The delayed signal "fires" a 2D21 thyratron, which produces a positive output pulse of approximately 350 volts. The 50,000 ohm potentiometer in the cathode circuit controls the sensitivity of this thyratron circuit. The 350 volt pulse from the 2D21 is used to "fire" a 6279 hydrogen thyratron. When the hydrogen thyratron conducts, 30,000 volts is made available to the triggered spark gap by the pulser-cable. In the above arrangement, two thyratrons are used, rather than one, in order to keep voltage across the time delay at a sufficiently low value.

The hydrogen thyratron and the pulser-cable arrangement is an adaptation of circuitry published by Theophanis (1960). The pulser-cable is made from 24 feet of RG-58/U coaxial cable, and is initially charged to 15,000 volts. When the hydrogen thyratron conducts, a 30,000 volt pulse is produced across A and B. The 15,000 volts is applied to the thyratron by a small, 15,000 volt, 5 ma power supply that is manufactured by Plastic Capacitors, Inc. It was found that the ends of the pulser-cable could not be connected by means of high-voltage coaxial connectors, as a short would occur. The positive and negative terminals had to be separated. The pulser-cable arrangement is advantageous in that it allows the polarity of the pulse to the triggered gap to be reversed by reversing the output leads.

The time delay is set in the following manner. Switch, S, is

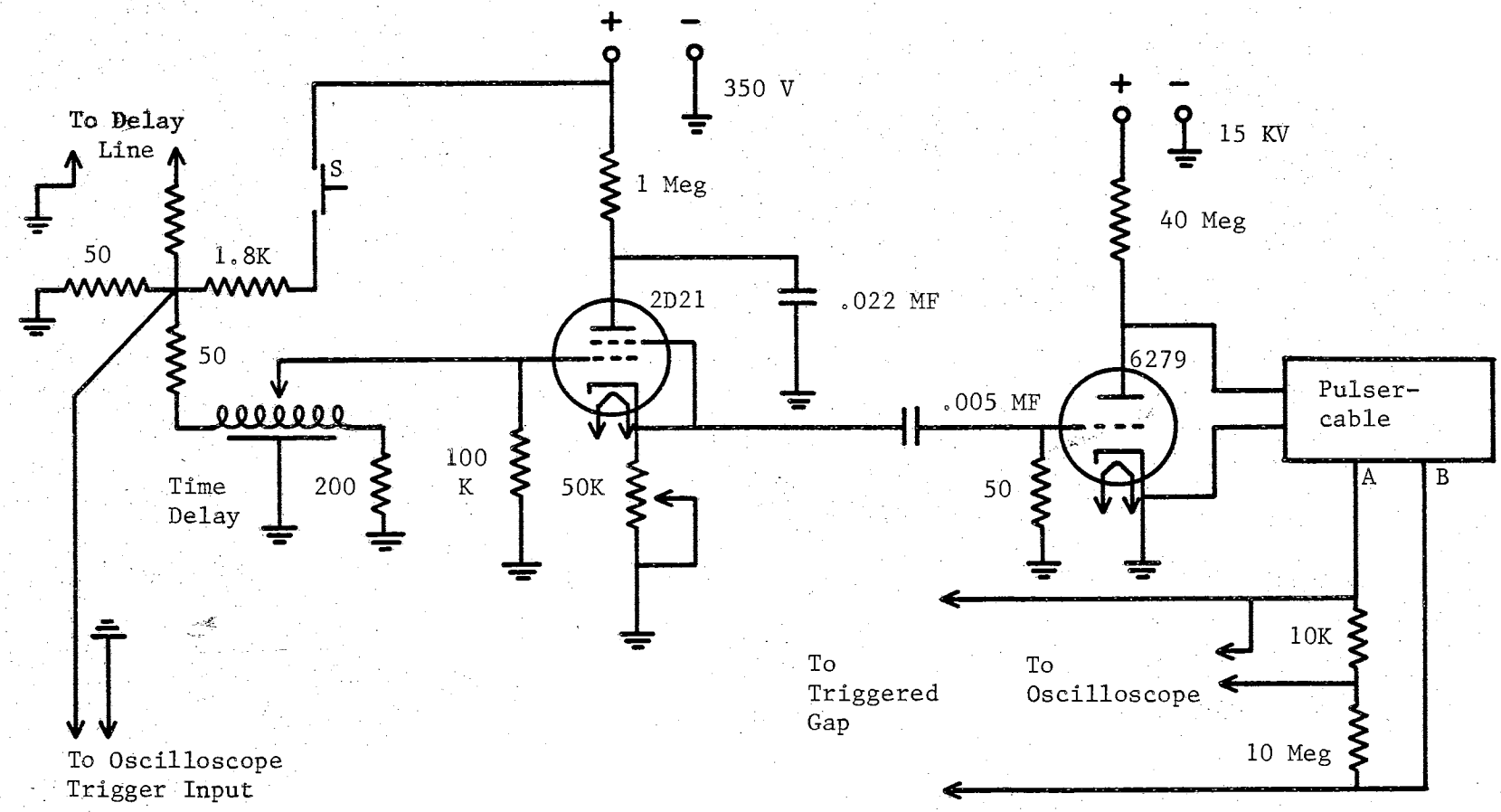

Figure 19. Time Delay and Thyratron Pulser

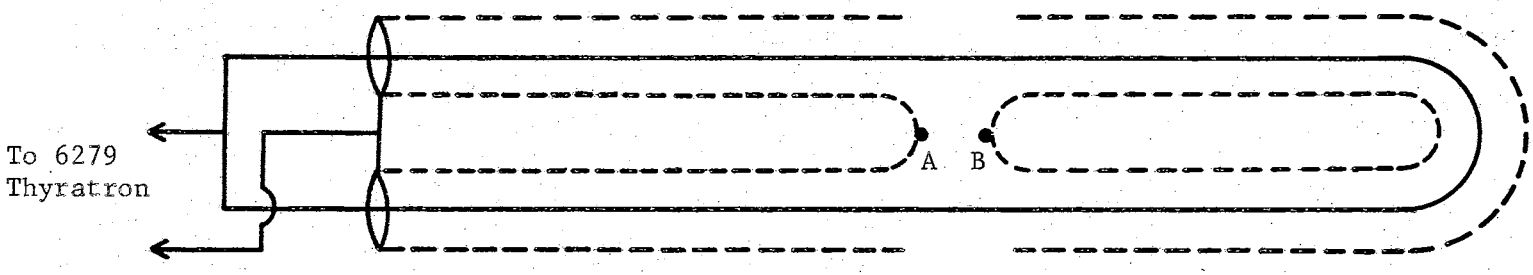

Figure 20. Pulser-cable

closed. This applies a small step voltage to the trigger input of the oscilloscope, causing the electron beam to begin its trace. At the same time, a step voltage is applied to the time delay. After a time interval of duration, t_d, 30,000 volts appears across A and B. Part of this voltage is applied to the vertical input of the oscilloscope. Thus, a pulse is seen on the oscilloscope at a time, t_d, after the electton beam begins its trace. The variable time delay is adjusted until the correct value of t_d is obtained. The correct value is approximately 5.7 microseconds, which is the time for the pulse to propagate from the switching gap to the wire and back to the triggered gap.

The Nitrogen System

The gas in the spark gaps of the "exploding wire" system is nitrogen. This gas is employed because it is readily available in bottled form, and because it does not support oxidation of the spark gap electrodes. The nitrogen is fed to a manifold (Figure 21). where its distribution is controlled by high pressure valves. The pressure is determined by a regulator that is mounted on the gas bottle.

Attached to the bottom of the manifold is a solenoid exhaust valve, which is activated by a 30 volt power supply. After the spark gaps have been filled with nitrogen to the proper pressure, the valve to the switching gap is opened, leaving all others closed. Activation of the solenoid valve releases the pressure from the switching gap, and the voltage falls until the voltage of the pulse generator causes the gap to break down.

In order to prevent circulating currents in the "exploding wire" system, metal tubing is not used to distribute the nitrogen. Instead,

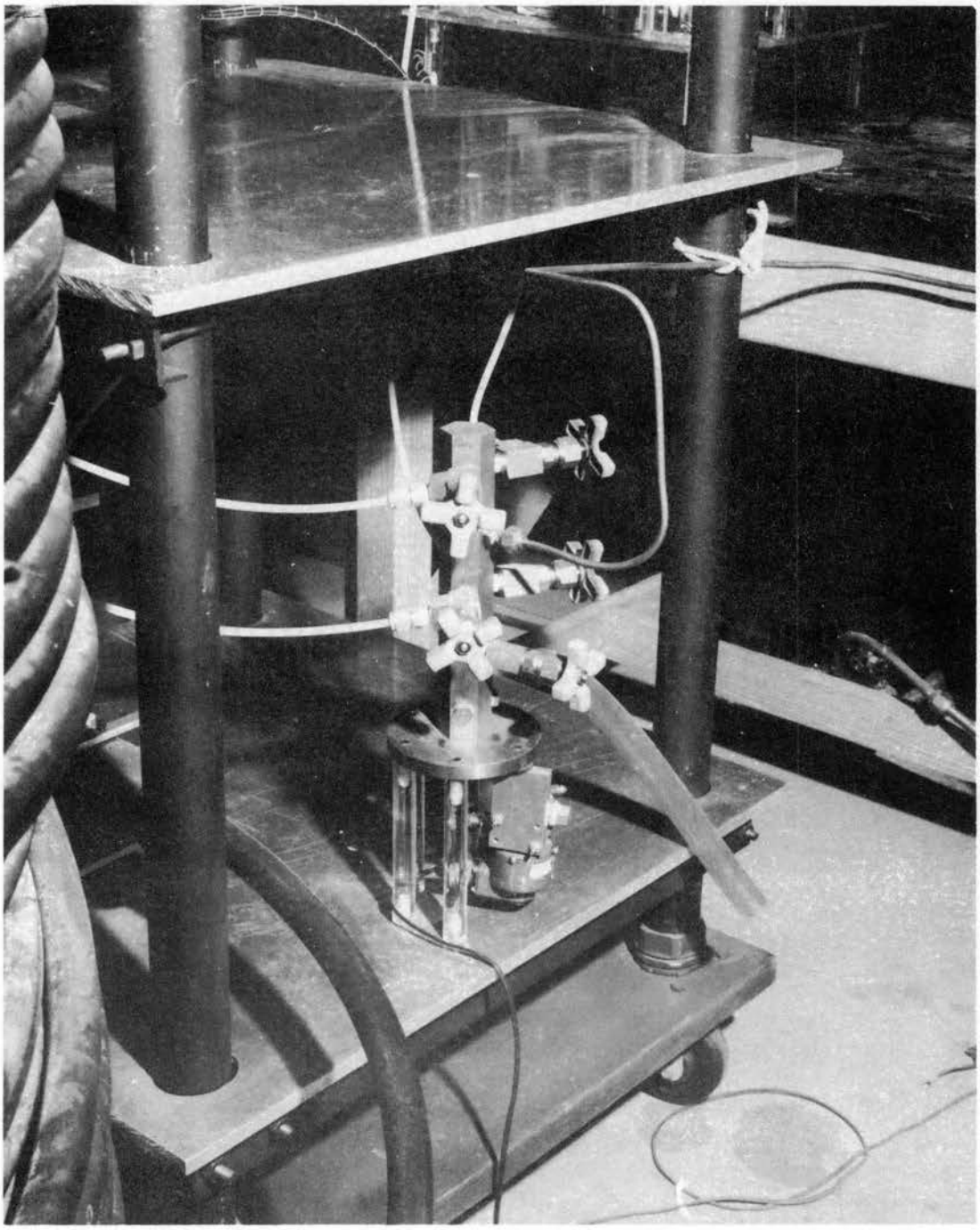

Figure 21. Photograph of Pressure Manifold

1/4 inch, high pressure nylon tubing is used. This tubing is rated at 3000 psi, and is connected by means of standard high pressure stainless steel pipe fittings. Circulating currents are further averted by mounting all metal parts on a three-deck aluminum table by means of lucite rods. This construction is clearly seen in Figure 21.

In Chapter IV, the general form of Paschen's curve was discussed. Paschen's curve for high pressure nitrogen is presented in Figure 22. The minimum of the curve cannot be seen on this scale. This curve is derived from two sources. Below a breakdown voltage of 9000 volts, the curve is obtained from the experimental data of Williams (1959). The upper range is obtained by applying Raether's criterion, $(\alpha\, d)_c = 20$. The calculations were made in the following manner. First, a value of P d is selected, and then α_c/P is calculated by the equation,

$$\alpha_c/P = 20/P\ d.$$

A value of E/P is found from the curve for the coefficient of ionization for nitrogen given by Cobine (1958). This curve is presented in Figure 23. Finally, the breakdown voltage, V_b, is calculated from the equation,

$$E/P = V_b/P\ d.$$

It should be remembered that the Paschen's curve is only accurate to within perhaps 10 per cent in its upper range. This should be sufficient for initial setting of the spark gap electrodes. Ultimately, the electrode separation of the spark gaps is determined by experiment.

The Explosion Chamber

In designing the chamber in which the wire is exploded, several

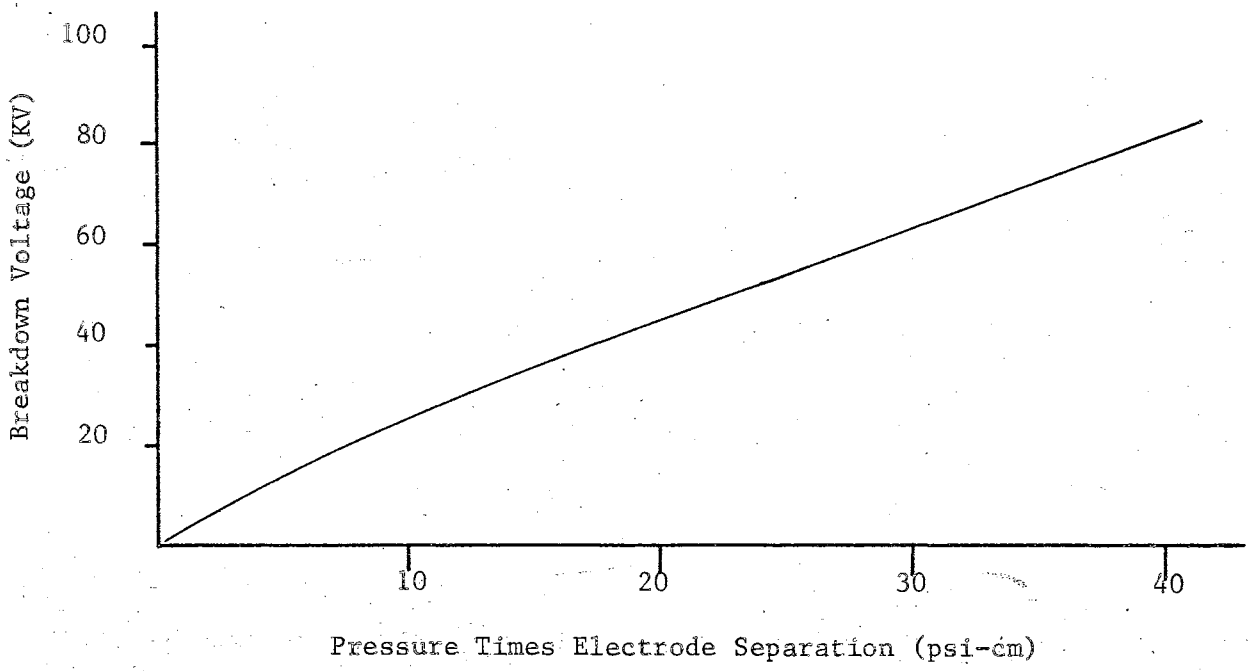

Figure 22. Paschen's Curve for Nitrogen

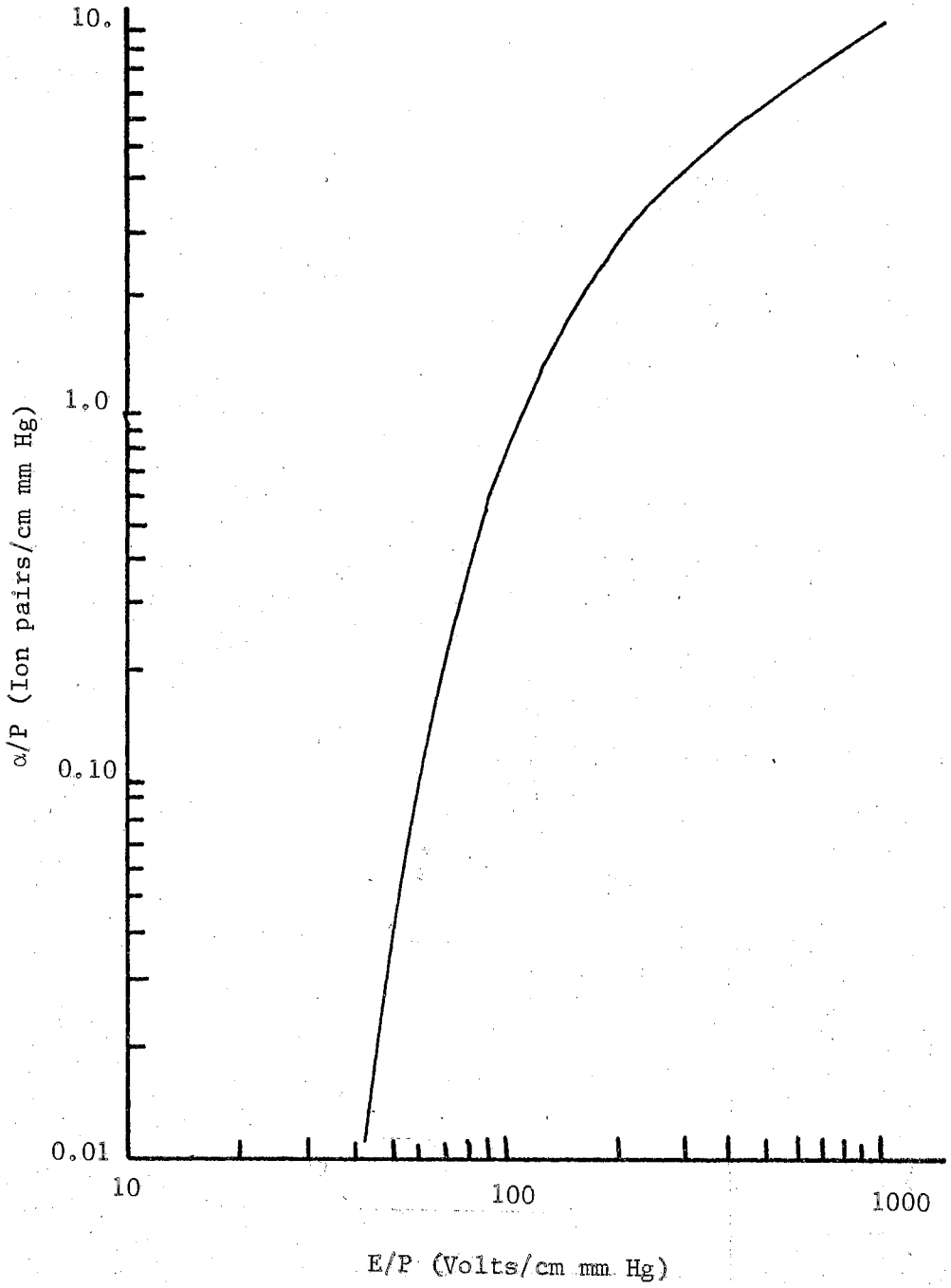

Figure 23. Coefficient of Ionization for Nitrogen

qualifications are stipulated:

1. The explosion is to take place in a vacuum.
2. The chamber is to be impedance-matched to the RG-19A/U cable.
3. The current is to be delivered symmetrically to the wire so that no unbalanced forces are produced.
4. Ports are to be provided for observation and experimentation.
5. A means of measuring the voltage variation with time across the wire is to be provided.

Following the preceeding guides, the chamber that is illustrated in Figure 24 was designed and constructed. A photograph of the chamber appears in Figure 25. The main body of the chamber is made of cold rolled brass and is constructed in two parts. In this way, the chamber may be disassembled for insertion of a wire. The two halves are sealed by an "O" ring. The center conductor, which introduces current into the chamber, is made of cold rolled brass and is silver plated, as is also the interior of the chamber. The insulator, which holds the center conductor, is made of high density polyethelene. It is force-fitted in place so as to form a vacuum seal.

Four ports surround the position of the "exploding wire. Two of these are windows and are made of pyrex glass. This construction is illustrated at the top of Figure 24. A third port, similar in construction to the window ports, is connected to a vacuum diffusion pump through a 1.5 foot section of stainless steel pipe. Part of this construction is seen in Figure 25. Four inches outside the chamber, this pipe has a joint so the chamber may be disconnected from the vacuum system. A fourth port, illustrated at the bottom of Figure 24, is larger than the other three. This port is used for insertion of probes, for the

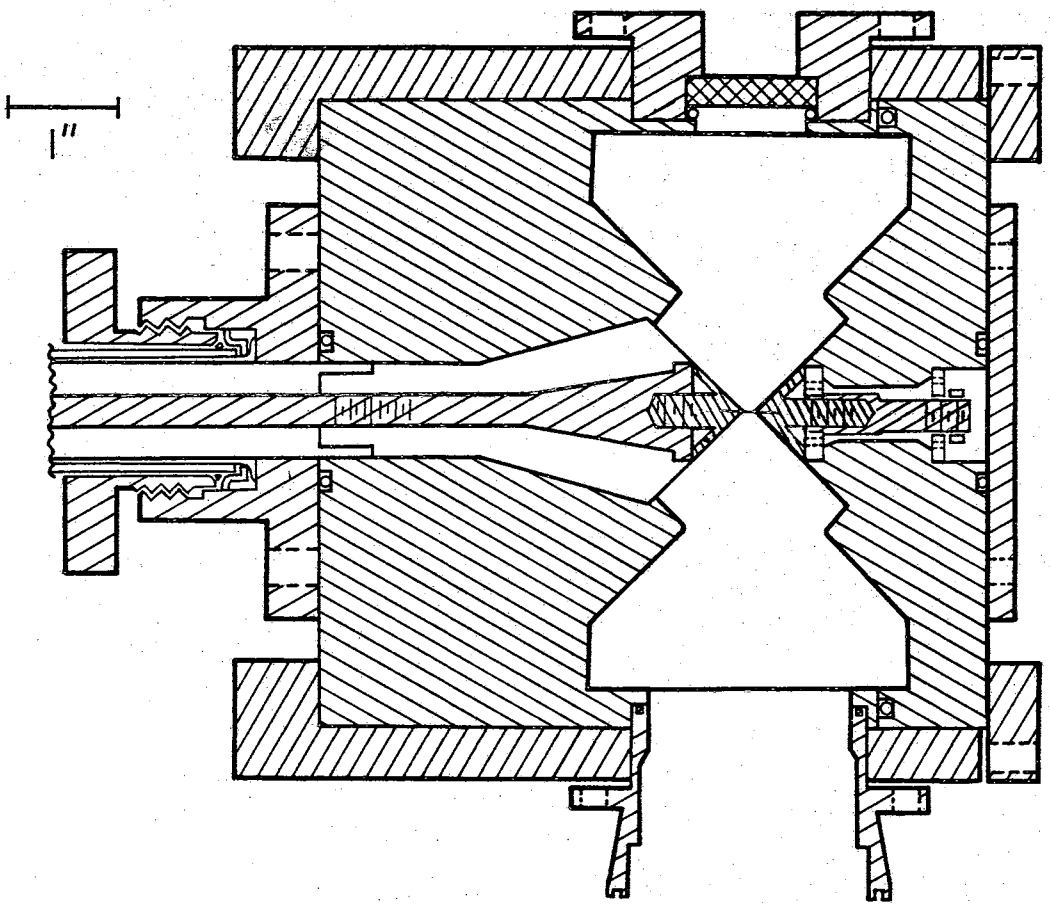

Figure 24. Explosion Chamber

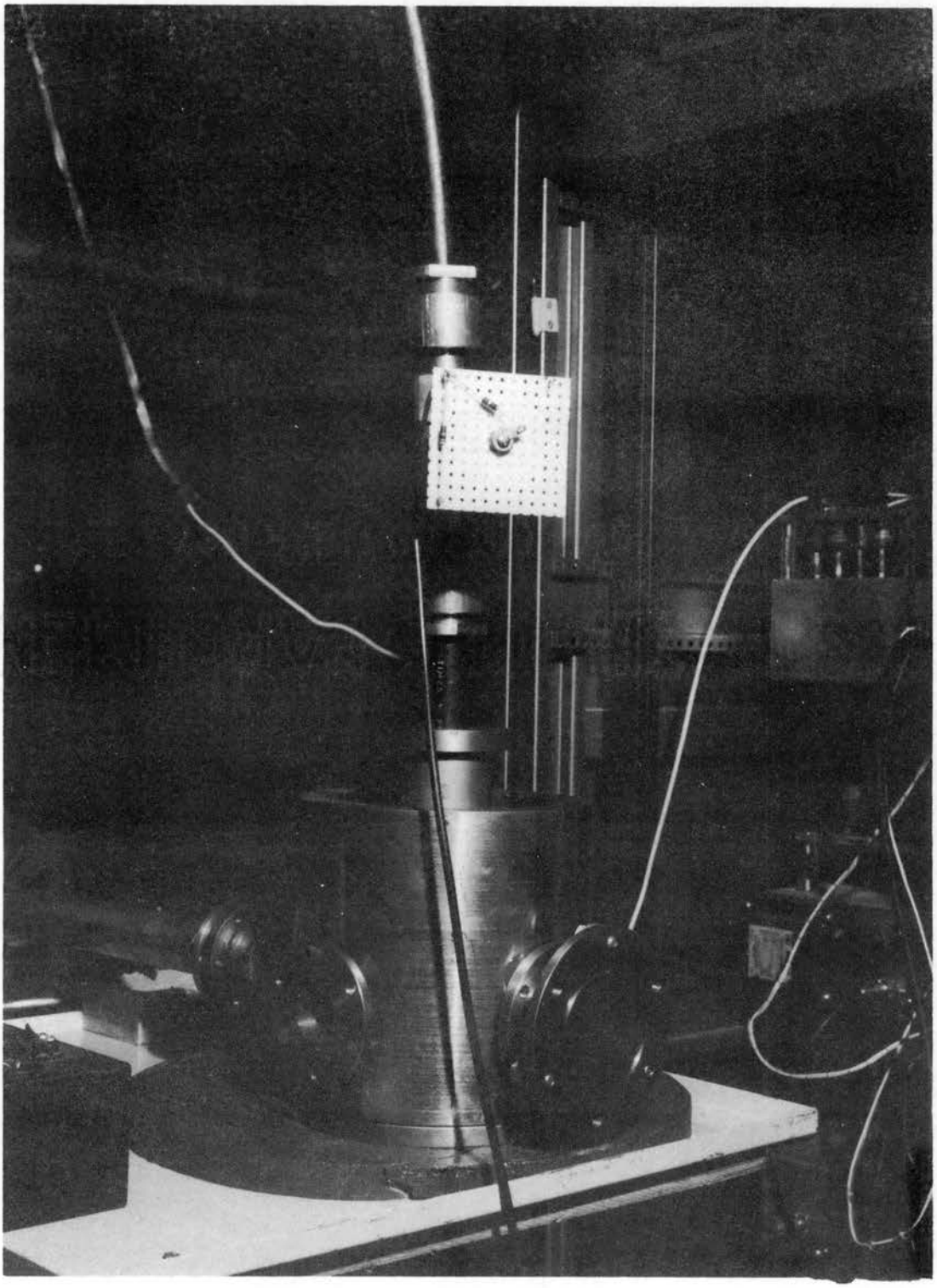

Figure 25. Photograph of Explosion Chamber

quadrupole mass filter and for other experimental devices to measure the properties of the plasma. When not in use, this port is covered with a plate.

The explosion chamber is connected to the pulse shaping gap by a 10 foot section of RG-19A/U cable. This length of cable allows the chamber to be moved aobut without causing the cable to bind. A "T" connection is provided on this cable just outside the chamber. A voltage divider is mounted on a circuit board, across the inner and outer conductors of this "T". This construction may be seen the the photograph, Figure 25. This voltage divider is connected to an oscilloscope through a section of RG-58/U cable, where the voltage across the wire is measured.

In order to hold the wire, special wire holders had to be disigned. The final disign is illustrated in Figure 26. The wire holder is made of copper, and is made in a conical shape. The apex angle of the cone is 90°. A 0.004 inches slot is cut through the apex, along the axis of the holder. Two holes, 1/16 inch in diameter, are bored at right angle to one another and at right angle to the axis of the cone. The bottom of the slot corresponds to the hole, A - B. A wire is installed in the left hand holder of Figure 24 in the following manner. First, the small section of the body of the chamber is removed. The holder is partially screwed into it mount. A wire is brought down through the slot so that it lies in hole, A - B. A rod, about 1/32 inch in diameter, is inserted through the hole, C - D, above the wire. The wire is held at one end, the other end is pulled so that it is alligned along the axis of the holder, and the holder is tightened into its mount. The wire is pinched held at the apex because of the tabs on the washer, made of shim stock, beneath the holder. These tabs are alligned at 90° to the axis of the

slot. The wire is installed in the other holder in a similar manner. But, the holder is tightened to its mount by a nut outside the main cavity of the caamber. The wire is pulled taut through the port illustrated at the bottom of Figure 24. Excess wire is easily removed from the holders by pulling on it. This breaks the wire somewhere inside the holders.

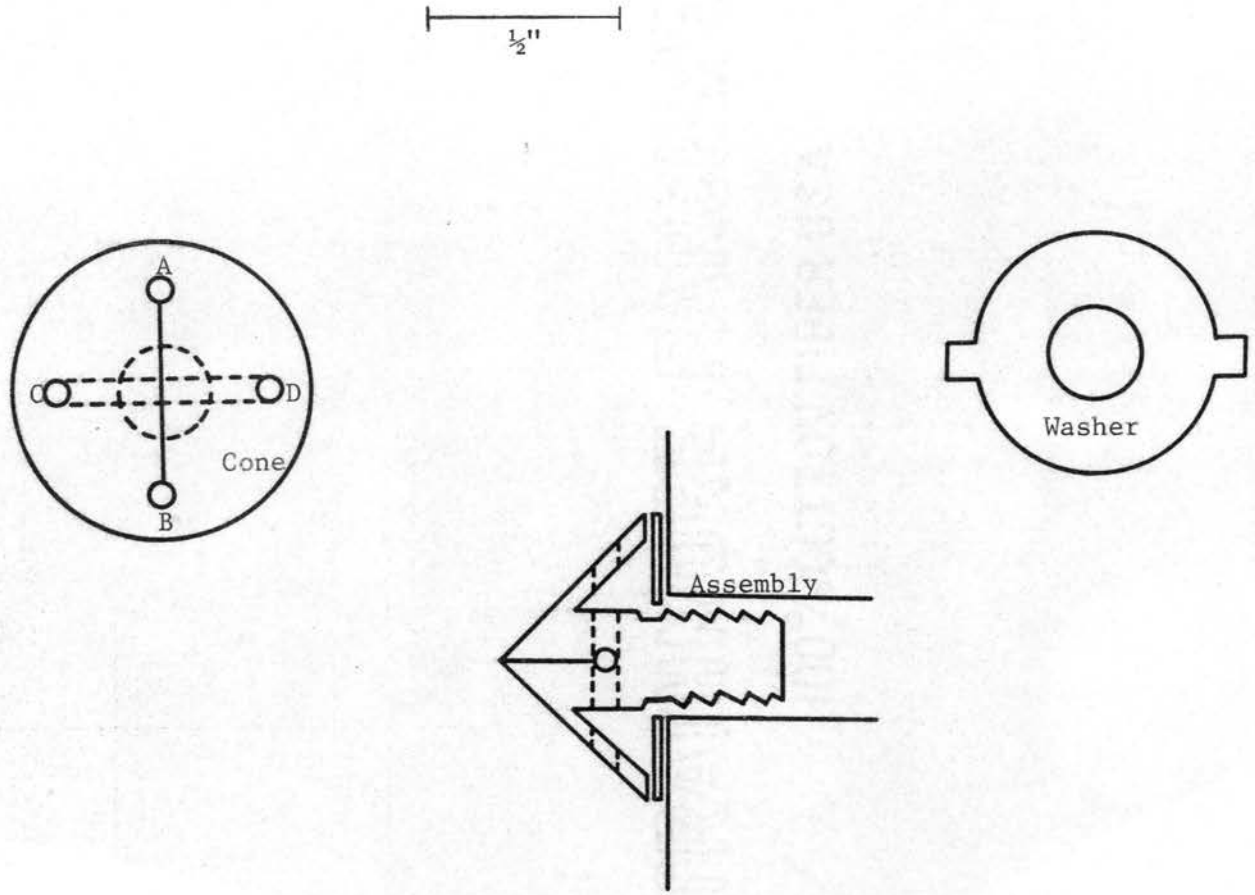

Figure 26. Wire Holder Assimbly

CHAPTER VI

PRELIMINARY RESULTS

The primary objective of the project for this thesis is to design and construct an "exploding wire" system that is capable of producing a high energy-density, aluminum plasma. The plasma is to have an initial density near to that of solid aluminum and is to expand from this density into a vacuum which is free of electromagnetic fields. In this final chapter, some preliminary results are presented on the performance of this equipment. Wires have been exploded with the pulse generator charged to 52,000 volts, which gives a pulse of 26,000 volts. This is roughly 19 per cent of the energy rating of the equipment. Several difficulties were encountered. Improvements are suggested.

Explosion Characteristics

In this section, results are given for wires exploded with low and medium voltages on the pulse generator. In the two cases which are discussed, the switching gap was set to "fire" in the neighborhood of 100 psi. The pulse shaping gap was operated at atmospheric pressure. In the first case it was completely closed, and in the second case the electrodes were separated about 0.020 inches. In both cases the fore pump lowered the explosion chamber pressure to about 1 micron of Hg.

Little difficulty was encountered in exploding a wire with the

pulse generator charged to 13,600 volts. In this case, the wire was not mounted in the manner that is indicated in the preceeding chapter. The wire was held by clamping it behind the two holders. This was necessary since the holders were not yet completely fabricated at that time. The length of the aluminum wire was about 1 inch and had a diameter of 0.001 inches. The voltage across the wire was measured as a function of time. This voltage variation with time is shown in Figure 27. A similar test was conducted with no wire and the holders removed. In this case, a square voltage pulse is expected across the open end of the delay line. The pulse, which was measured, is indicated in Figure 28. From the curve of Figure 27 and a knowledge of the amplitude of the voltage pulse, the resistance, power and energy were calculated as a function of time. A computer program was assembled to perform the calculations. The data points from the voltage curve, which were employed for the calculations, were selected in such a manner so the curve between any two points was a straight line. From the calculations, a curve was drawn which gives the relation between the resistance and the energy. This curve is shown in Figure 29.

Difficulties were encountered when a wire was exploded with the pulse generator charged to 52,000 volts. The pulse generator appeared to have a leakage path, as the generator would hold the voltage for only 10 to 20 seconds after it was disconnected from the power supply. Another difficulty was that of obtaining an oscilloscope trace. The electron beam would begin its sweep across the oscilloscope face before the wire began to receive energy, causing nothing but "trash" on the oscilloscope face. Evidently, the electromagnetic radiation from the "firing" of the switching gap caused the oscilloscope to trigger

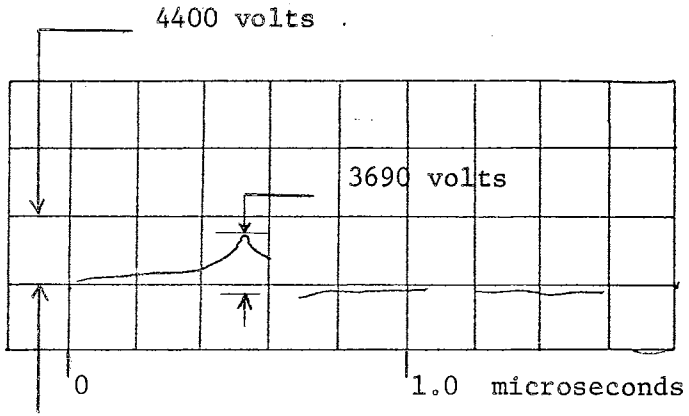

Wire
Material: Aluminum
Diameter: 0.001 inches
Length: approx. 1 inch

Pulse Voltage: 6,800 volts

Figure 27. Voltage vs. Time for a 0.001 Inches Wire

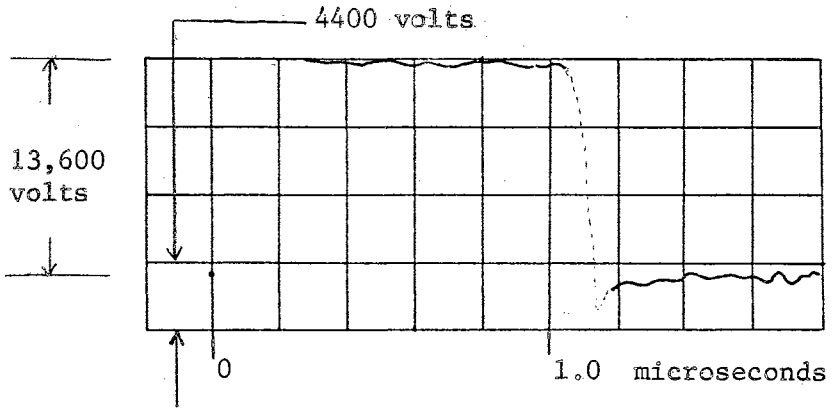

Wire: None

Figure 28. Square Voltage Pulse

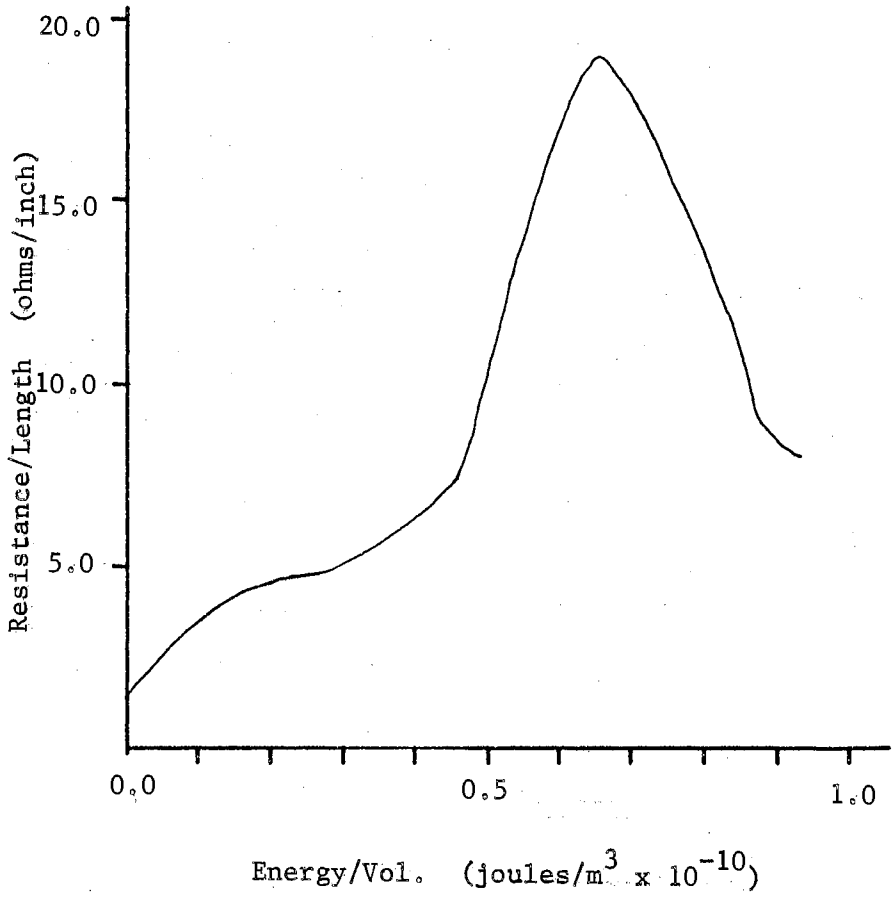

Figure 29. Resistance vs. Energy for a 0.001 Inches Aluminum Wire

prematurely. To alleviate this second situation, the internal delay of the oscilloscope was used. The stray radiation triggered the delay. After an appropriate delay, the oscilloscope made a single sweep.

Employing the delayed sweep, a 0.002 inches diameter wire, about 1/4 inch in length, was exploded. The pulse generator was charged to 52,000 volts, as indicated by a high voltage probe which was connected to a vacuum tube voltmeter. The high voltage power supply for charging the "condenser" cable was disconnected from the cable after the solenoid valve was activated. This allowed perhaps one and not more than two seconds for leakage to discharge the pulse generator. To allow for a slight leakage, a value of 22,000 volts was assumed for the amplitude of the voltage pulse in the calculations. The oscillographic trace of the variation of the voltage across the wire is shown in Figure 30. A curve for the resistance versus energy for this experiment is presented in Figure 31.

The results for the preceeding two experiments, which have been discussed, are similar in several respects. The initial rate a wire absorbs energy from the voltage pulse is proportional to the quantity, V^2 L/A, where V is the voltage to which the pulse generator is charged, L is the length of the wire and A is the cross sectional area of the wire. In both of the experiments, this quantity is approximately the same. This indicates that the energy absorbed by the wires should be of the same order of magnitude.

In both experiments, a dominant feature is evident. This is the existence of a voltage peak. At this voltage peak, the resistance of the wire becomes a maximum, the current through the wire becomes a minimum, and the rate of insertion of energy into the wire becomes a

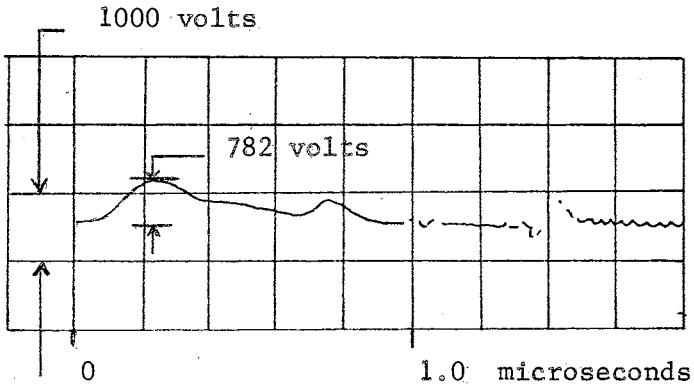

Wire
Material: Aluminum
Diameter: 0.002 inches
Length: approx. 1/4 inch

Pulse Voltage: 26,000 volts

Figure 30. Voltage vs. Time for a 0.002 Inches Wire

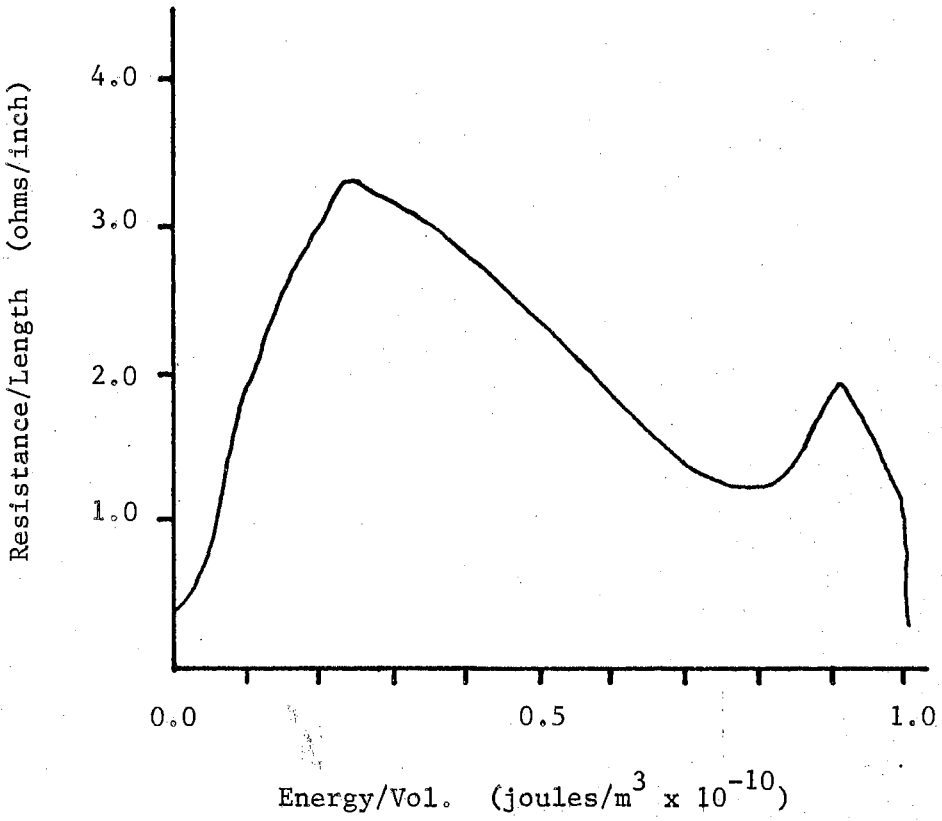

Figure 31. Resistance vs. Energy for a 0.002 Inches Aluminum Wire

maximum.

Very interesting situations occur for both experiments at an energy density of approximately 0.9×10^{10} joules/m^3. In the first experiment, the resistance of the wire suddenly drops to zero. In the second experiment, the resistance reaches a secondary peak, and then very sharply decreases to zero. Additional experiments are required before the exact nature of this sudden voltage drop is determined.

The Triggered Gap

The electronic circuitry for "firing" the triggered gap was tested. To do this, two alligator clips were clipped to a piece of plexiglass and separated about 1/4 inch. This arrangement served as a spark gap. It was found that the gap would consistently spark-over when the test switch, S, of Figure 19 was closed. No attempt has yet been made to test the triggered spark gap in the "dynamic" situation. It was believed that time could be better spent in working the "bugs" out of the other parts of the system.

Wire Length

In using the "exploding wire" system, the ability to accurately determine the energy density in the wire, or the plasma, is very important. A means of measuring the length of the wire becomes very important for this purpose. The following method accomplishes this objective. The joint between the two halves of the explosion chamber serves as a reference line for measuring distances. A thick washer with a conical hole is fabricated to fit over the wire holder in the large section of the explosion chamber. A flat surface on the washer is perpendicular to

the axis of the wire holder. A measurement is taken between the reference line and the flat surface of the washer, using a depth gauge. A second measurement is made from the outer surface of the small section of the explosion chamber to a flat surface on the screw which holds the other wire holder. A knowledge of these measured distances and the dimentions of the various parts of the explosion chamber serve to determine the length of the wire.

Spark Gap Leakage

The spark gaps, which have been designed, should be able to contain a high pressure gas without much leakage. If a leak exists, long exposure to high pressures may result in a sufficiently high leakage so the leak may be located. The spark gaps were measured for leakage. It was determined that the leakage rate was on the order of 10 psi per minute at 1000 psi. This rate is sufficiently slow to allow experiments to be performed without concern for the variation in the spark gap pressure with time.

If two more pressure regulators were employed, no variation of pressure would occur in the gaps. Valves would be provided to exhaust the gaps when not in use. The present pressure manifold would be used with the present solenoid valve on the switching gap.

Wire Holders

The wire holders, as designed, seem to work very well. It was found that these holders were capable of holding wires of diameter, 0.0007 inches .

Suggestions for Improvements

Problems encountered during the course of the project suggest several improvements. Of primary importance is the elimination of the leakage from the pulse generator. When this difficulty is resolved, an accurate determination of the amplitude of the voltage pulse is possible.

A second improvement, as indicated earlier, is to establish separate regulation for the pressure in each of the spark gaps.

In addition to the preceeding improvements, the following two tasks are to be performed:

1. Place the triggered gap into operation.
2. Determine the optimum pressures and the optimum electrode separations for the spark gaps.

When the improvements, mentioned in this section, have been accomplished, the system should be ready for making significant measurements of the plasma by exploding wires at high energy densities.

A SELECTED BIBLIOGRAPHY

Acker, F. E. and G. W. Penney. "Some Experimental Observations of the Propagation of Streamers in the "Low Field" Regions of an Asymmetric Gap." Journal of Applied Physics, Vol. 40 (1969), 2397.

Anderson et. al. APPENDIX to "Solid and Solid-Liquid Phases in Wires at High Current Densities." by M. E. Meeker, Sandia Corp. Tech. Memo. 314-58 (51), Aug., 1958.

Bennett, F. D. "Exploding Wires." Sci. Am., Vol. 206, #5 (1962), 102.

Bennett, F. D. "High Temperature Cores in Exploding Wires." Physics of Fluids, Vol. 8 (1965), 1106.

Brown, Vernon D. "Use of a Pulsed Photomultiplier to Measure the Light Intensity versus Time for a Spark Discharge Between Aluminum Electrodes." (unpublished Ph.D. dissertation, Oklahoma State University, 1968).

Bruce, R. E. "A Model and Calculations for the Properties of an Exploding Plasma Sphere." (unpublished Ph.D. dissertation, Oklahoma State University, 1966).

Cobine, J. D. Gaseous Conductors, New York: Dover Publications, Inc., 1958.

Fletcher, R. C. "Production of Ultra-High Speed Impulses." Rev. Sci. Instr., Vol. 20 (1949), 861.

Francis, G. Ionization Phenomena in Gases, New York: Academic Press, 1960.

Frungel, F. B. A. High Speed Pulse Technology, Vol. 1, New York: Academic Press, 1965.

Gartenhaus, S. Elements of Plasma Physics, New York: Holt, Rinehart, Winston, Inc., 1964.

Hague, B. The Principles of Electromagnetism Applied to Electrical Machines, New York: Dover Publications, Inc., 1962.

Jahnke, E. and F. Emde. Tables of Functions with Formulas and Curves, New York: Dover Publications, Inc., 1943.

Kells, L. M. Elementary Differential Equations, New York: McGraw-Hill Book Co., Inc., 1960.

King, A. L. Thermophysics, San Francisco: W. H. Freeman and Co., 1962.

Kvartskhava, I. F. et. al. "Oscillographic Determination of Energy of Electric Explosion of Wires." Soviet Phys. JETP, Vol. 4 (1957), 623.

Meek, J. M. and J. D. Craggs. Electrical Breakdown of Gases, London: Oxford at the Clarendon Press, 1953.

Millman, J. and H. Taub. Pulse and Digital Circuits, New York: McGraw-Hill Book Co., Inc., 1956.

Oliver, F. W. J. "Bessel Functions of Integer Order." Handbook of Mathematical Functions with Formulas Graphs, and Mathematical Tables, ed. M. Abramowitz and I. A. Stegun. Washington D. C.: U.S. Dept. of Commerce, National Bureau of Standards, 1965.

Papoular, R. Electrical Phenomena in Gases, New York: American Elsevier Publishing CO., 1965.

Payne, R. D. and F. C. Todd. "A Spectrograph for the Far-ultraviolet." Proc. Okla. Acad. Sci., Vol. 46 (1966), 115.

Peek, F. W. Dielectric Phenomena in High-Voltage Engineering, New York: McGraw-Hill Book Co., Inc., 1929.

Reithel, R. J. and J. H. Blackburn. "A Hydrodynamic Explanation for the Anomalous Resistance of Exploding Wires." Exploding Wires, Vol. 2, ed. W. G. Chase and H. K. Moore. New York: Plenum Press, 1962.

Theophanis, G. A. "Millimicrosecond Triggering of High Voltage Spark Gaps." Rev. Sci. Instr., Vol. 31 (1960), 427.

Thomas, R. J. and J. R. Hearst. "An Electronic Scheme fpr Measuring Exploding Wire Energy." IEEE Transactions on Instruments and Measurement, Vol. IM-16 (1967), 51.

Tucker, T. J. and F. W. Neilson. "The Electrical Behavior of Fine Wires Exploded by a Coaxial Cable Discharge System." Sandia Corp. Reprint SCR-92, May, 1959.

Tucker, T. J. "Square-Wave Generator for the Study of Exploding Wires." Rev. Sci. Instr., Vol. 31 (1960), 165.

Van Kampen, N. G. and B. U. Felderhof. Theoretical Methods in Plasma Physics, New York: John Wiley & Sons, Inc., 1967.

Whitmer, R. M. Electromagnetics, Inglewood Cliffs, N. J.: Prentice-Hall, Inc., 1962.

Williams, T. J. "The Theory and Design of the Triggered Spark Gap." Sandia Corp. Tech. Memo. SCTM 186-59-(14), May, 1959.

Willis, H. W. "Quadrupole Mass Filter Design and Construction for Plasma Ion Analysis." (Published M.S. thesis, Oklahoma State University, 1969).

APPENDIX A

PROPERTIES OF BESSEL FUNCTIONS

The following properties of Bessel functions were needed in the solution of the differential equations for the "pinch effect" and are taken from Kells (1960).

Let $J_n(x)$ be the Bessel function of order n with argument x. Then, the relationship between Bessel functions of different orders is

$$J_n'(x) = -J_{n+1}(x) + (n/x)\, J_n(x)$$
$$J_n'(x) = J_{n-1}(x) - (n/x)\, J_n(x) \ .$$

Integrals of Bessel functions of different orders are related by the equation,

$$\int_0^P x^k\, J_{n+1}(ax)\, dx = ((n+k)/a) \int_0^P x^{k-1}\, J_n(ax)\, dx - (P^k/a)\, J_n(aP) \quad ; \ k \geq 1$$

The orthogonality condition for Bessel functions is

$$\int_0^1 x\, J_n(ax)\, J_n(bx)\, dx = \tfrac{1}{2}\, J_n'^2(b)\, \delta_{ab}$$

where a and b are roots of $J_n(x) = 0$.

APPENDIX B

POLYNOMIAL APPROXIMATION FOR BESSEL FUNCTIONS OF ORDER ZERO

In the computer calculations for the "pinch effect", the following polynomial approximation for Bessel functions of order zero, due to Oliver (1965), was used.

Let x be the argument of the Bessel function of order zero, J_o. Then for

$$-3 \leq x \leq 3,$$

the approximations is

$$J_o(x) = \sum_{n=0}^{6} C_n y^{2n} + \varepsilon$$

where $y = x/3$ and

$$C_o = 1.0$$
$$C_1 = -2.2499997$$
$$C_2 = 1.2656208$$
$$C_3 = -0.3163866$$
$$C_4 = 0.0444479$$
$$C_5 = -0.0039444$$
$$C_6 = 0.0002100$$

The accuracy of this approximation is determined by

$$|\varepsilon| < 5 \times 10^{-8}$$

For

$$3 \leq x < \infty,$$

the approximation is

$$J_o(x) = x^{-\frac{1}{2}} f_o \cos(\theta_o),$$

where

$$f_o = \sum_{n=0}^{6} D_n y^n + \varepsilon_1$$

$$\theta_0 = x + \sum_{n=0}^{6} E_n y^n + \varepsilon_2$$

$$y = 3/x$$

and

$$D_o = 0.79788456$$

$$D_1 = -0.00000077$$

$$D_2 = -0.00552740$$

$$D_3 = -0.00009512$$

$$D_4 = 0.00137237$$

$$D_5 = -0.00072805$$

$$D_6 = 0.00014476$$

$$E_o = -0.78539816$$

$$E_1 = -0.04166397$$

$$E_2 = -0.00003954$$

$$E_3 = 0.00262573$$

$$E_4 = -0.00054125$$

$$E_5 = -0.00029333$$

$$E_6 = 0.00013558$$

The accuracy of this approximation is determined by

$$|\varepsilon_1| < 1.6 \times 10^{-8}$$
$$|\varepsilon_2| < 7 \times 10^{-8}.$$

APPENDIX C

PARAMETERS FOR THE RG-19A/U COAXIAL CABLE

Below are given the various parameters for the RG-19A/U coaxial cable. Some of the parameters were taken from the specification sheet for the cable; others were calculated from the equations given in TABLE II. Using the same notation as in Table II, these parameters are:

$A = 0.250$ in

$B = 0.910$ in

$k = 2.24$

$C_L = 29.5$ pf/ft

$H_L = 78.8$ mhy/ft

$R_o = 52$ ohms

$v = 587$ ft/μsec .

VITA

Jerry Allen Yoder

Candidate for the Degree of

Master of Science

Thesis: THEORY, DESIGN, AND PERFORMANCE OF A COAXIAL, EXPLODING-WIRE SYSTEM

Major Field: Physics

Biographical:

Personal Data: Born the eldest son of Mr. and Mrs. Monroe E. Yoder, March 7, 1942, at New California, Ohio.

Education: Graduated from Dublin High School, Dublin, Ohio, in May, 1960; attended Ohio Valley College, Parkersburg, West Virginia, from September, 1960 to May 1962; received the Bachelor of Arts degree in Physics from Oklahoma City University, Oklahoma City, Oklahoma, in May, 1964; completed the requirements for the Master of Science degree in Physics at Oklahoma State University, Stillwater, Oklahoma, in May, 1970.

Professional Experience: Laboratory Teaching Assistant at Oklahoma City University during senior year; recipient of NASA Traineeship for the three years beginning with September, 1964, at Oklahoma State University; served as a Graduate Teaching Assistant for the Physics Department and as a Graduate Research Assistant for the Research Foundation, both of Oklahoma State University; charter member of Sigma Pi Sigma at Oklahoma City University; member of the Oklahoma Academy of Science.